Advances in Polymer Technology

Polymer Materials Processing in Microstructure

Lead Guest Editor: Bin Xu
Guest Editors: Dazhi Sun and Yongkai Yin,

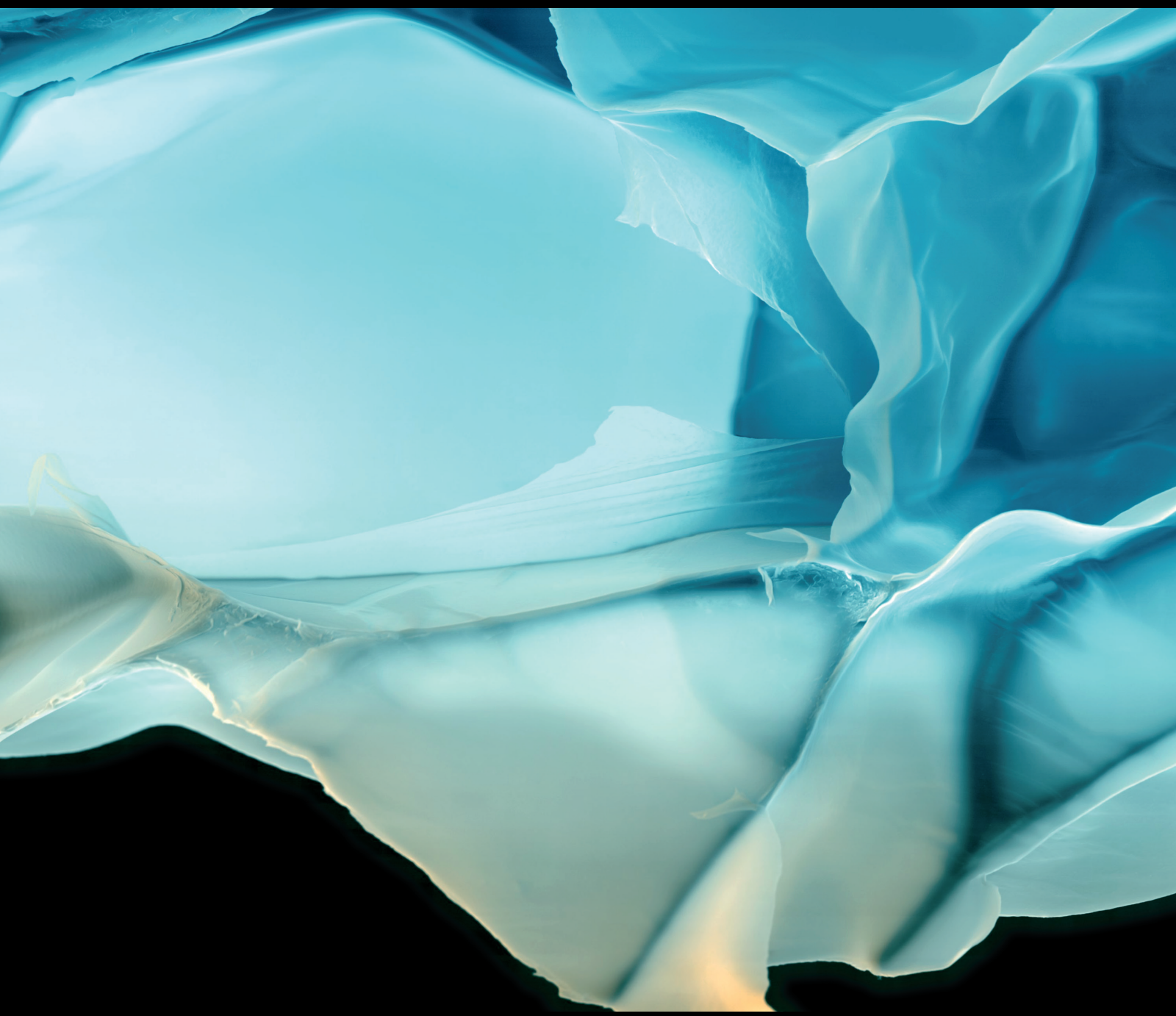

Polymer Materials Processing in Microstructure

Advances in Polymer Technology

Polymer Materials Processing in Microstructure

Lead Guest Editor: Bin Xu
Guest Editors: Dazhi Sun and Yongkai Yin,

Contents

Hindawi
Advances in Polymer Technology
Volume 2019, Article ID 9859506, 11 pages
https://doi.org/10.1155/2019/9859506

Research Article

Emulsion Electrospun Fiber Mats of PCL/PVA/Chitosan and Eugenol for Wound Dressing Applications

Cláudia Mouro,[1] **Manuel Simões**,[2] **and Isabel C. Gouveia**[1]

[1]*FibEnTech Research Unit, Faculty of Engineering, University of Beira Interior, Covilhã 6201-001, Portugal*
[2]*LEPABE—Department of Chemical Engineering, Faculty of Engineering of University of Porto, Porto 4200-465, Portugal*

Correspondence should be addressed to Isabel C. Gouveia; igouveia@ubi.pt

Received 3 May 2019; Accepted 7 July 2019; Published 30 October 2019

Guest Editor: Bin Xu

In recent years, the damaging effects of antimicrobial resistance relating to wound management and infections have driven the ongoing development of composite wound dressing mats containing natural compounds, such as plant extracts and their derivatives. The present research reports the fabrication of novel electrospun Polycaprolactone (PCL)/Polyvinyl Alcohol (PVA)/Chitosan (CS) fiber mats loaded with Eugenol (EUG), an essential oil, known for its therapeutic properties. The electrospun fiber mats were prepared via electrospinning from either water-in-oil (W/O) or oil-in-water (O/W) emulsions and characterized using scanning electron microscopy (SEM), Fourier-transform infrared spectroscopy (FT-IR), total porosity measurements, and water contact angle. The *in vitro* EUG release profile and antibacterial activity against *Staphylococcus aureus* and *Pseudomonas aeruginosa* were also evaluated. The obtained results proved that the EUG was loaded efficiently into electrospun PCL/PVA/CS fiber mats and the two W/O and O/W emulsions prepared from the PCL/PVA/CS (7 : 3 : 1) and PCL/PVA/CS (3 : 7 : 1) revealed porosity within the ideal range of 60–90%, even when EUG was loaded. The measured contact angle values showed that the O/W emulsion exhibited a more hydrophilic character and the wettability noticeably decreased after adding EUG in both emulsion blends. Furthermore, the electrospun PCL/PVA/CS fiber mats demonstrated a rapid release of EUG during the first 8 hours, which enhanced gradually afterward (up to 120 hours). Moreover, an efficient antibacterial activity against *S. aureus* (inhibition ratios of 92.43% and 83.08%) and *P. aeruginosa* (inhibition ratios of 94.68% and 87.85%) was displayed and the *in vitro* cytotoxic assay demonstrated that the normal human dermal fibroblasts (NHDF) remained viable for at least 7 days, after direct contact with the produced electrospun fiber mats. Therefore, such findings support the biocompatibility and suitability of using these EUG-loaded electrospun PCL/PVA/CS fiber mats as a new innovative wound dressing material with potential for preventing and treating microbial wound infections.

1. Introduction

The integrity of the skin can be affected by several disorders. When the skin is injured, it becomes more susceptible to microbial infections, which can have negative consequences on the healing process [1, 2]. Therefore, the development of materials with suitable barrier properties using different antimicrobial agents have shown to prevent and suppress the microbial invasion and colonization by pathogenic bacteria [3]. However, it is still a challenge to achieve the release of these agents directly onto the damaged tissue to ensure the correct therapeutic dosage and prevent the wound from getting infections.

Recently, composite wound dressing mats produced by electrospinning have attracted research attention due to their unique properties like extremely high surface area, high porosity, and small pore size [4, 5]. In addition, these materials are known in the wound management field for their capability to absorb excess exudate from the wound, while they create and maintain a moist environment. Moreover, electrospun fiber mats provide wound protection from mechanical trauma and bacterial colonization, exhibit high air, and oxygen permeability, as well as mimic the properties of natural extracellular matrix (ECM) ensuring additional support for cell growth and proliferation in order to promote the wound healing with the minimum scar formation [4–6]. Also, electrospinning has the ability to incorporate different types of bioactive or therapeutic agents, thus leading to the enhancing of the desirable wound healing properties [6]. Antibiotics, growth factors (GFs), vitamins, antimicrobial, analgesics, and anti-inflammatory compounds are among the most successful bioactive agents so far loaded into electrospun fiber mats [7]. Nevertheless,

medicinal plant extracts, and their derivatives, such as essential oils, have captured the attention of researchers due to their traditional therapeutic properties, cost-effectiveness, and availability [6].

Eugenol (EUG), a naturally occurring phenolic component extracted from cloves, is known for its analgesic, antimicrobial, antioxidant, anti-inflammatory, and anticarcinogenic properties and has demonstrated abilities to improve the healing process and tissue regeneration [8–10]. However, EUG presents poor water solubility, and its stability can be affected by chemical and enzymatic degradation, losses by volatilization or thermal decomposition [11, 12]. In order to overcome EUG disadvantages, emulsion electrospinning is of particular interest to successfully incorporate both hydrophilic and hydrophobic bioactive agents, while preventing the loss of their structural integrity and bioactivity [13].

Emulsion electrospinning is a novel and straightforward technique similar to the traditional electrospinning, where water-in-oil (W/O) or oil-in-water (O/W) emulsions are used instead of a conventional polymer solution [14, 15]. This modified electrospinning method does not require a special apparatus, neither a careful selection of the operating conditions to ensure desirable results. In addition, emulsion electrospinning has been used to improve the solubility of poorly soluble bioactive agents and, consequently, their therapeutic effectiveness. Furthermore, this approach also increases the affinity of the oil and water phases and plays a significant role in the stability of low molecular weight polymers and diluted polymer solutions [13].

In this context, the present work describes the innovative development of EUG-loaded into electrospun Polycaprolactone (PCL)/Polyvinyl Alcohol (PVA)/Chitosan (CS) fiber mats through W/O and O/W emulsions by nanospider technology, a needle-free electrospinning equipment, based on a rotating spinning electrode immersed into a liquid polymer bath. The modern nanospider technology differs from conventional electrospinning because it allows the formation of many taylor cones (the source of nanofibers) simultaneously on the surface of the rotating spinning electrode, and hence this technology is highly productive and more effective to produce high-quality nanofibers [16, 17].

In this way, a nontoxic hydrophobic synthetic polymer, PCL, known for its many advantages over the main synthetic polymers was used to act as a protective barrier against external threats. However, the data available in the literature showed that cells are more prone to adhere, proliferate, and grow on a moderate hydrophilic surface than on a hydrophobic or super-hydrophilic surface [18, 19]. Therefore, CS, a naturally occurring polysaccharide, was selected for its abilities, namely by supporting cell adhesion and growth of several cell types and also by exhibiting hemostatic and antimicrobial properties [20]. Nevertheless, CS is difficult to electrospun into a fibrous structure and exhibits low mechanical properties, which restricts its use in medical applications [21, 22]. To overcome these limitations, CS has been blended with other biocompatible hydrophilic synthetic polymers, like PVA [23]. Herein, in this study, CS and PVA were blended in order to ensure efficient exudate management and provide a moist wound environment. Moreover, the PVA/CS blend exhibits an inhibitory effect on microbial growth and promote cell adhesion and proliferation [24]. The biological abilities of EUG, mainly analgesic, anti-inflammatory, and antimicrobial properties have also been exploited to strengthen the healing process.

Therefore, we present new findings claiming the development of new EUG-loaded electrospun PCL/PVA/CS fiber mats prepared from W/O and O/W emulsions, for wound dressing applications. The results obtained revealed that mixing PCL, PVA, and CS enhanced the final properties of the blend. CS formed miscible blends with PVA, which acted as a good emulsifying and dispersing agent and made CS/PVA blend compatible with the PCL. The antimicrobial and non-cytotoxic effect of EUG was also seen as a promising strategy to develop new innovative wound dressings, with the potential to prevent and treat microbial-resistant wound infections.

2. Materials and Methods

2.1. Materials. Polycaprolactone (PCL) (MW 80.000 g/mol) and Chitosan (CS) (MW 50.000–190.000 g/mol, degree of deacetylation 75–85%) and Eugenol (EUG) were purchased from Sigma-Aldrich. Polyvinyl Alcohol (PVA) (MW 115.000 g/mol) was purchased from VWR Chemicals. Chloroform (analytical grade), Dimethylformamide (DMF) (analytical grade), Glacial acetic acid, and Ethanol absolute were purchased from Fisher Chemical. Normal human dermal fibroblasts (NHDF) cells were acquired from ATCC—American Type Culture Collection. Brain Heart Infusion (BHI) Broth was provided from Panreac. Nutrient Agar (NA), Nutrient Broth (NB), and Agar for microbiology were purchased from Fluka. Sodium chloride (NaCl), Mueller-Hinton Broth (MHB), Dimethyl sulfoxide (DMSO) anhydrous ≥99.9%, Tween 80, Trysin, and 3-(4,5-Dimethyl-2-thiazolyl)-2,5-diphenyl-2H-tetrazolium bromide (MTT) were purchased from Sigma Aldrich. Phosphate-buffered saline (PBS), pH 7.4 was purchased from Alfa Aesar. All solvents were used as received without further purification.

2.2. Determination of Minimum Inhibitory Concentration (MIC) of EUG. Minimal Inhibitory Concentration (MIC) of EUG was applied against two bacterial strains: *Staphylococcus aureus* ATTC 6538 and *Pseudomonas aeruginosa* PA25 by the broth microdilution method according to NCLS M07-A6 guidelines. Briefly, EUG stock solution was prepared in DMSO (10% (v/v)) to yield a concentration of 20 μL/mL. Serial dilutions of EUG were made in MHB with concentrations ranging from 10 to 1 μL/mL. Then, overnight liquid bacterial cultures were adjusted to 0.5 McFarland turbidity standards with sterile water. Afterward, bacterial work suspensions were formed from 500 μL of the 0.5 McFarland suspensions and 4500 μL of MHB. A volume of 50 μL of bacterial work suspensions and 50 μL of the EUG dilutions were added into 96 multi-well polystyrene plates (Sigma-Aldrich). The multi-well plates were incubated for 24 hours at 37°C. Deposited bacteria (dot-shaped) in the bottom of each well were evaluated. The last well in the dilution series that showed deposit (bacterial killing) corresponded to MIC of EUG. All the determinations were performed in triplicate.

2.3. Preparation of Electrospinning Emulsions. PCL solution (8% w/v) was prepared by dissolving PCL in chloroform/DMF (volume ratio of 30 : 20) at 50°C under magnetic stirring until complete dissolution. Afterward, the solution was left to stir overnight to ensure proper dissolution of the PCL before being blended with the PVA/CS blend. CS solution (4% w/v) was prepared by dissolving CS in acetic acid (14%) at room temperature. Also, a PVA solution (10% w/v) in distilled water was prepared at 90°C. PVA and CS solutions were then mixed in two different ratios, 7 : 1 and 3 : 1 (v/v), to form the PVA/CS blend solution. The W/O emulsion blend 8% PCL/10% PVA/4% CS (7 : 3 : 1) was prepared by simultaneous adding of PVA/CS blend solution to PCL solution, followed by mixing with high-speed homogenizer (Techmatic S2), while the O/W emulsion blend 8% PCL/10% PVA/4% CS) (3 : 7 : 1) was prepared by simultaneous adding of PCL solution to PVA/CS blend solution. The final mixtures were stirred at room temperature for 4 hours to ensure complete dissolution and to obtain uniform emulsions. PCL/PVA/CS blends were also loaded with EUG. The final concentration of the EUG was 5% (w/w) (based on the weight of the PCL powder), i.e., 5% over the weight of the fiber (owf) EUG. All emulsions were immediately used for electrospinning.

2.4. Electrospinning . The stable and homogenous emulsions were electrospun using Nanospider Technology (Nanospider laboratory machine NS LAB 500S from Elmarco s.r.o., Cezek Republic, http://www.elmarco.com). Electrospinning of the emulsions was carried out with a distance between the spinning electrode and collecting electrode of 13 cm at a driving voltage of 75.0 kV and a rotating spinning electrode of 9.6 rpm (60 HZ). The collection time was ~1.0 hour at 25°C and relative humidity up to 35%. The electrospun fiber mats were collected on polypropylene nonwoven fabric and were dried in the hood at room temperature till constant weight. The same electrospinning conditions were used to pure PCL and PVA/CS blend as a reference for electrospun PCL/PVA/CS fiber mats with and without loaded EUG.

2.5. Electrospun Fiber Mats Characterization

2.5.1. Fourier Transform Infrared Spectroscopy (FT-IR). The chemical composition of pure PCL, PVA/CS, and electrospun PCL/PVA/CS fiber mats with and without loaded EUG were analysed on FT-IR. Measurements were performed on Thermo-Nicolet is10 FT-IR spectrophotometer over the range 500–4000 cm^{-1} with a spatial frequency resolution of 4 cm^{-1} and each sample was scanned 64 times.

2.5.2. Surface Morphology of Electrospun Fiber Mats. The surface morphology of the electrospun PCL/PVA/CS fiber mats with and without loaded EUG was investigated with the help of scanning electron microscope (SEM) Hitachi S2700 at a high voltage of 20 kV. The fiber diameters were directly measured from SEM images using public domain software (Image J, National Institutes of Health, USA). After that, the average diameter and diameter distribution were determined by applying SPSS Statistics 21.0 software (SPSS Inc. Chicago, USA).

2.5.3. Porosity Measurement. The total porosity of the dry electrospun fiber mats was measured using a liquid displacement method, as described by Chitrattha et al. [25]. Ethanol was used as the displacement liquid because it readily penetrated into the pores of the matrices and did not induce shrinkage or swelling of these materials. Briefly, a preweighed porous membrane (W_s) was immersed in a cylinder containing 20 mL of ethanol (W_1) and placed in a water sonicator bath (Ultrasons-H, P-Selecta) for 40 min at 30°C to assist the penetration of ethanol into the porous structure. Subsequently, the volume in the sonicated cylinder containing porous membrane impregnated with ethanol was readjusted to 20 mL and weighed (W_2). After that, the membrane saturated with ethanol was removed from the cylinder and the cylinder was reweighed (W_3). The porosity (ε) of these porous materials was determined using the following Equation (1) [25]:

$$\varepsilon(\%) = \left(W_2 - W_3 - W_s\right)/\left(W_1 - W_3\right) \times 100. \quad (1)$$

2.5.4. Water Contact-Angle Determination. The surface wettability of pure PCL, PVA/CS, and electrospun PCL/PVA/CS fiber mats with and without loaded EUG were determined through water contact angle (WCA) using a data physics contact angle system OCAH-200 apparatus. To accomplish that, deionized water droplets were placed on the surface of each sample at room temperature and the contact angle was calculated after 10 s of incubation time to avoid discrepancy in the contact angle values measured. The measurements were conducted on different sample locations and the average was reported as the contact angle of each sample.

2.6. Release In Vitro of EUG from EUG-Loaded Electrospun PCL/PVA/CS Fiber Mats. Release of EUG from EUG-loaded electrospun PCL/PVA/CS fiber mats was studied by UV–Vis spectrometry. To perform this assay, standard solutions of EUG with concentrations from 0.00 μL/mL to 10.00 μL/mL were prepared and a calibration curve was drawn at 282 nm (maximum wavelength of EUG). Samples (2 × 2 cm) of EUG-loaded electrospun PCL/PVA/CS fiber mats were immersed in 10 mL of phosphate-buffered saline (PBS, pH = 7.4) at 37°C with constant rotation at a speed of 100 rpm. Afterward, 3 mL of release medium was recovered at specified time intervals, ranging between 0 and 120 hours, and at the same time, an equal volume of the fresh PBS solution was replenished to maintain a constant volume. The concentration of EUG that remained in the release medium at each time point was quantified at 282 nm using UV–Vis spectrophotometer. All measurements were carried out in triplicate.

2.7. Estimation of Antibacterial Activity of EUG-Loaded Electrospun PCL/PVA/CS Fiber Mats. The antibacterial effect of EUG loaded into electrospun PCL/PVA/CS fiber mats was carried out according to E 2180-07 standard test method for determining the activity of incorporated antimicrobial agent(s) in polymeric or hydrophobic materials. *S. aureus* and *P. aeruginosa* were selected, once they are the most common bacteria present in wound infections [26].

To perform the assay, a bacterial suspension ($1–5 \times 10^8$ CFU/mL) was added in an agar slurry previously prepared from 0.85 (w/v) NaCl and 0.3 (w/v) agar-agar in deionized water. Afterward, a thin layer of inoculated agar slurry was poured onto 3×3 cm square samples of electrospun PCL/PVA/CS fiber mats with and without EUG loaded. The samples were evaluated immediately after adding the inoculated agar slurry (T_{0h}) and after 18–24 hours in contact with the inoculated agar slurry at 37°C for 18–24 hours (T_{24h}). For each sample, serial dilutions of the agar slurry were done with 0.85 (w/v) NaCl, plated in agar plates, and incubated for 18–24 hours at 37°C. The antimicrobial efficiency was quantitatively expressed in percentage of bacterial reduction (%R) using Equation (2) by comparing the CFU on the control samples (electrospun PCL/PVA/CS fiber mats), C, with the CFU on the samples loaded with 5% owf EUG (5% EUG-loaded electrospun PCL/PVA/CS fiber mats), A [27].

$$\text{Percentage Reduction (\%R)} = ((C - A)/C) \times 100. \quad (2)$$

According to Japanese Industrial Standard JIS L 1902:2002, the bacteriostatic or bactericidal effect of the electrospun PCL/PVA/CS fiber mats containing EUG was then calculated using Equations (3) and (4):

$$\text{Bacteriostatic activity value} = M_B - M_C, \quad (3)$$

$$\text{Bactericidal activity value} = M_A - M_C, \quad (4)$$

where M_A is the average of the common logarithm of the number of living bacteria in control samples immediately after adding the inoculated agar slurry (T_{0h}), M_B is the average of the common logarithm of the number of living bacteria in control samples after 18–24 hours in contact with the inoculated agar slurry (T_{24h}), and M_C is the average of the common logarithm of the number of living bacteria in samples containing 5% owf EUG after 18–24 hours in contact with the inoculated agar slurry (T_{24h}).

2.8. Characterization of the Cytotoxicity Profile of the EUG-Loaded Electrospun PCL/PVA/CS Fiber Mats. The cytotoxic profiles of the produced electrospun PCL/PVA/CS fiber mats with and without EUG were performed *in vitro* following ISO 10993–5 (Biological evaluation of medical devices-Part 5: Tests for in vitro cytotoxicity). Briefly, the samples were placed in 24-well plates (Sigma-Aldrich) at the center of each well occupying <1/10 of its area and then sterilized under UV irradiation (254 nm, ~7 mW cm^{-2}) for 1 hour. After that, normal human dermal fibroblast (NHDF) cells were used as a model to seed each well at a density of 1×10^4 cells/well and incubated at 37°C, in an incubator under a humidified atmosphere containing 5% CO_2. After an incubation period of 1, 3, and 7 days, the mitochondrial redox activity of the viable cells was assessed through the reduction of the MTT into an insoluble blue formazan dye. In this way, the medium of each well was removed and it was replaced with a mixture of fresh culture medium and the MTT reagent solution. After 4 hours of incubation at 37°C and 5% CO_2 humidified atmosphere, the MTT solution was removed and DMSO was added to each well in order to dissolve the formazan crystals. Finally, the absorbance of each sample was measured at 570 nm using a microplate reader (Biorad xMark microplate spectrophotometer). Wells containing cells cultured without the materials and wells containing cells cultured with EtOH (96%) were also included as a negative control (K^-) and positive control (K^+), respectively.

2.9. Statistical Analysis. Data were analyzed statistically by the one-way analysis of variance (ANOVA) and Tukey Post-Hoc test using SPSS 21.0 (SPSS Inc. Chicago, USA). Statistical calculations were based on a confidence level ≥95% (values of $P <; 0.05$ were considered statistically significant).

3. Results and Discussion

3.1. Determination of Minimum Inhibitory Concentration (MIC) of EUG. Minimal Inhibitory Concentration (MIC) of EUG against *S. aureus* and *P. aeruginosa* was found to be 4.25 μL/mL and 3.00 μL/mL, respectively. Several other studies have confirmed the significant antibacterial activity of EUG against *S. aureus* and *P. aeruginosa*. For example, Sanla-Ead et al. [28] described MIC of 25.00 μL/mL against *S. aureus* and 50.00 μL/mL against *P. aeruginosa,* which were higher than those found in this study. However, the MIC values for specific alkaloids obtained from plants, namely the bioactive properties of these natural compounds depend on various factors, including the environmental condition and seasonal variables, as well as the geographical location and method of extraction.

3.2. Electrospun Fiber Mats Characterization

3.2.1. Fourier Transform Infrared Spectroscopy (FT-IR). The FT-IR spectra of pure PCL, PVA/CS and electrospun PCL/PVA/CS fiber mats with and without EUG were acquired and represented in Figure 1. The FT-IR spectrum of pure PCL exhibits its characteristic peaks, Figures 1(a)(i) and 1(b)(i). Peaks at 2866.05 and 2945.76 cm^{-1} are attributed to symmetric and asymmetric CH_2 stretching vibrations. At 1722.51 cm^{-1} occurs an intense, sharp peak, which corresponds to carbonyl stretching vibration of the ester group, while the peaks at 1293.80, 1239.67, and 1164.76 cm^{-1} are associated for C-O and C-C stretching, asymmetric and symmetric–C-O-C stretching, respectively [29]. On the other hand, the characteristic bands of both PVA and CS are displayed in the FT-IR spectrum of the PVA/CS blend. Figures 1(a)(ii) and 1(b)(ii) shows the characteristic peaks at 1558.80 cm^{-1} and 1653.25 cm^{-1}, corresponding to N-H bending vibrations in secondary amides and C=O stretching vibrations of the amide bond, respectively. Moreover, the spectrum of PVA/CS blend exhibits a broad peak at 3118.56 cm^{-1}, which is assigned to O-H and N-H stretching.

Additionally, the emulsion blends of PCL/PVA/CS (Figures 1(a)(iii) and 1(b)(iii)) display a sharp peak at around 1720.00 cm^{-1} which corresponds to the PCL and a broad peak in the region between 3000 and 3500 cm^{-1} that belongs to PVA/CS blend. Likewise, the FT-IR spectra of electrospun

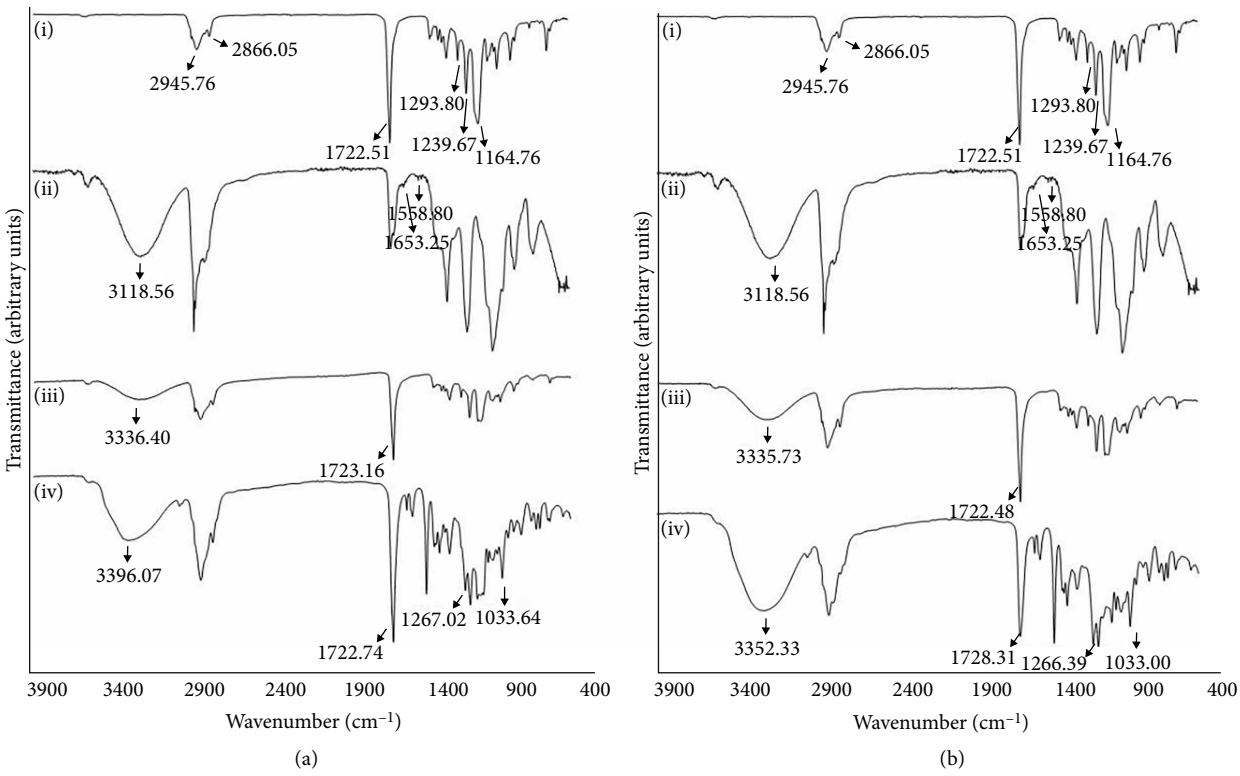

Figure 1: FT-IR spectrums of pure PCL (i), PVA/CS (ii) and electrospun PCL/PVA/CS fiber mats from W/O emulsion (a) and from O/W emulsion (b). Electrospun PCL/PVA/CS fiber mats without loaded EUG (iii) and with 5% owf EUG (iv).

PCL/PVA/CS fiber mats containing EUG (Figures 1(a)(iv) and 1(b)(iv)) exhibit those peaks and other characteristic peaks at around 1033.00 and 1267.00 cm^{-1}, regarding the stretching vibration of symmetric and asymmetric C-O-C, which demonstrate the presence of the methoxy group of EUG. Moreover, the presence of all characteristic peaks of the components used to produce the electrospun fiber mats proves the successful blending of the EUG with the PCL/PVA/CS emulsions.

However, the FT-IR analysis suggests that there is no evidence of chemical bonding between each component of the blend because new absorption peaks are not seen in FT-IR spectra. Nevertheless, some chemical interactions could have occurred among carboxyl, amino, and hydroxyl groups of the PCL, PVA, CS, and bioactive agent. These interactions can be suggested by slight displacement of absorption peaks, as well as by different peak intensities and peak widths.

Similar results were presented by Ajalloueian et al. [20]. The FT-IR spectrum of PLGA/CS/PVA nanofibers displayed the characteristic peaks of PLGA, CS, and PVA, and when they removed the PVA from the blend fewer hydroxyl groups were detected as shown by a narrower and shorter peak at 3400–3700 cm^{-1}. Furthermore, Zargham et al. [19] demonstrated by FT-IR that olive oil was successfully embedded within the PCL/Olive oil composite nanofibers. Nevertheless, in the FT-IR spectrum of the PEO/CS/PCL/Olive oil composite nanofibers were not evident chemical bonding between the PEO/CS and PCL/Olive oil.

3.2.2. Surface Morphology of Electrospun Fiber Mats. SEM micrographs and fiber diameter distributions of EUG-loaded electrospun PCL/PVA/CS fiber mats, prepared via electrospinning from either W/O or O/W emulsions, are shown in Figure 2. The electrospun PCL/PVA/CS fiber mats produced from W/O emulsion displayed beads and fibers, known as the spindles or bead-on-a-string morphologies, with an average diameter of 379.05 ± 161.95 nm, Figure 2(a). When 5% owf EUG was incorporated, nanofibers with similar morphology were produced with a mean diameter of 387.07 ± 179.51 nm, Figure 2(b). In turn, the electrospun PCL/PVA/CS fiber mats produced from O/W emulsion, with and without EUG loaded, demonstrated thinner and more uniform fibers with fewer beads, with an average diameter of 174.47 ± 38.93 nm and 199.90 ± 48.86 nm, Figures 2(c) and 2(d), respectively. It showed that the PVA, which acts as an emulsifying agent, is the most critical component of the blend which controls the process of emulsion electrospinning [30]. Thus, PVA decreases the surface tension between immiscible phases and contributes towards the formation of more uniform nanofibers [30, 31]. Moreover, the O/W emulsions are especially useful for controlled or sustained release of the oil-soluble bioactive compounds, as the EUG.

Hajiali et al. [32] obtained similar results to Sodium Alginate (SA)-Polyethylene Oxide (PEO) nanofibers and SA-PEO containing 5% v/v of Lavender oil nanofibers. In both cases, 85% of fibers exhibited diameters in the range of 50–125 nm, with a most representative percentage between 75 and 100 nm. This result confirmed that the addition of

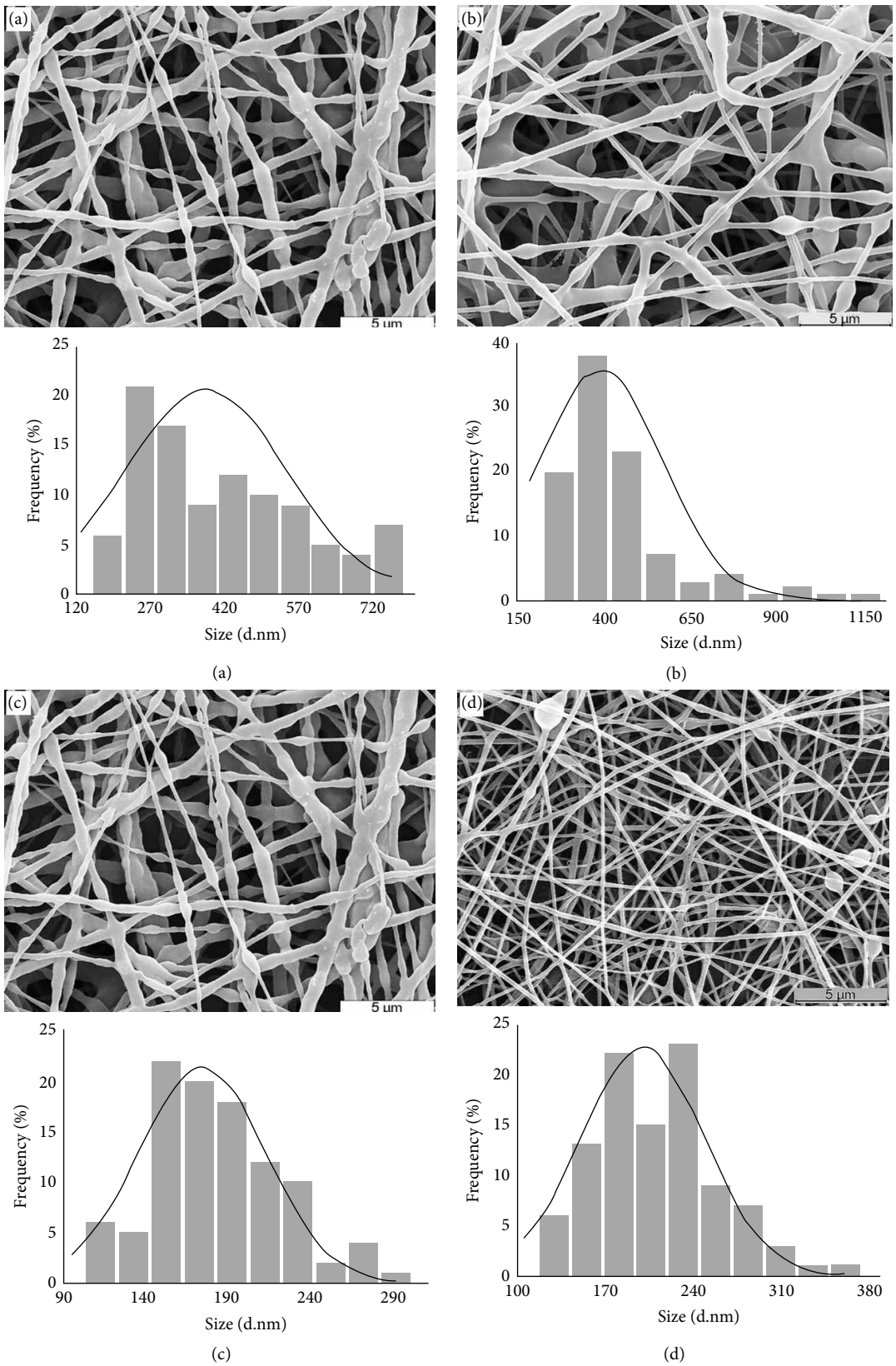

Figure 2: SEM images with fiber diameters distribution obtained from electrospun (a) PCL/PVA/CS fiber mats prepared via W/O emulsion without EUG loaded, (b) and with 5% owf EUG, (c) PCL/PVA/CS fiber mats prepared via O/W emulsion without EUG loaded, (d) and with 5% owf EUG.

essential oil to the polymer solution did not have a significant effect on fiber diameters.

Moreover, Gholipour-Kanani et al. [33] produced PCL/PVA/CS nanofibrous mats by adding PVA to PCL/CS in 2 : 1 : 1.33 (PCL/PVA/CS) blend ratio and obtained uniform fibers with diameters in the range of 136 ± 37.00 nm. This study revealed a mean diameter lower than the average diameter of fibers found for PCL/PVA/CS (7 : 3 : 1) (379.05 ± 161.95 nm) and PCL/PVA/CS (3 : 7 : 1) (174.47 ± 38.93 nm), confirming that both the composition and ratio of each component in the blend influence the fiber diameters.

3.2.3. Porosity Measurement. The wound dressings' porosity contributes to a correct gas, nutrient, and fluid exchange, as well as drug release. The porosity of a material is also essential to support cell adhesion and proliferation in the wound site [25].

Herein, the electrospun PCL/PVA/CS fiber mats produced from W/O and O/W emulsions presented a total porosity of 88.74 ± 2.27% and 90.46 ± 2.15%, respectively, as demonstrated in Table 1. The porosity values slightly decreased when the ratio of PCL in the emulsion blend increased, namely to W/O emulsion, and when EUG was loaded. Moreover, the electrospun PCL/PVA/CS fiber mats prepared from W/O emulsion loaded with EUG exhibited a total porosity of 84.44 ± 3.10%, while a value of 88.52 ± 4.09% was observed from the O/W emulsion loaded with EUG.

The total porosity values of the electrospun PCL/PVA/CS fiber mats, with and without EUG, are within the preferred range of 60–90% for an effective wound healing process [34]. Indeed, the high porosity exhibited by the produced electrospun fiber mats is more proper to provide a suitable pore structure for cell migration, nutrient exchange, and development of a new ECM, although it depends on the wound characteristics and the aim of wound management [25].

3.2.4. Water Contact-Angle Determination. Surface wettability of electrospun fiber mats is one of the most desirable material properties to the wound dressing applications, which may influence the initial adhesion and migration of cells, as well as their proliferation to the wound site [29, 35]. Therefore, the contact angle between water droplets and the electrospun fiber mats (WCA) was determined to assess the wettability of the pure PCL, PVA/CS, and electrospun PCL/PVA/CS fiber mats with and without EUG (Figure 3).

In this study, a hydrophobic polymer, PCL, 90.2 ± 7.30°, was blended with a hydrophilic polymer PVA/CS blend, 28.8 ± 5.50°, to improve the hydrophilic features of electrospinning emulsions [36]. WCA values of 61.2 ± 4.24° and 42.85 ± 3.95° were obtained for electrospun PCL/PVA/CS fiber mats prepared from W/O and O/W emulsions, respectively. The O/W emulsion presented a more hydrophilic character than W/O emulsion, due to inherent hydrophilic nature of both PVA and CS. However, the incorporation of EUG through the electrospun fiber mats was more hydrophobic. WCA values of 70.70 ± 4.62° and 59.37 ± 5.11° were displayed for electrospun PCL/PVA/CS fiber mats loaded with 5% owf EUG from W/O and O/W emulsions, respectively. Hence, the addition of EUG improves the most hydrophilic character of the O/W emulsion.

Table 1: Porosity measurement of electrospun PCL/PVA/CS fiber mats with and without loaded EUG.

Samples	Porosity (%)
W/O emulsion blend PCL/PVA/CS	88.74 ± 2.27
W/O emulsion blend PCL/PVA/CS + 5% owf EUG	84.44 ± 3.10
O/W emulsion blend PCL/PVA/CS	90.46 ± 2.15
O/W emulsion blend PCL/PVA/CS + 5% owf EUG	88.52 ± 4.09

Similar results found by Cui et al. [35] showed that increasing the PVA-SbQ amount in comparison with the Zein amount resulted in a lower WCA. The reason for this was because Zein, a predominantly corn-based protein, exhibits a more hydrophobic character due to a higher amount of hydrophobic (nonpolar) amino acids than hydrophilic (polar) ones.

3.3. Release In Vitro of EUG from EUG-Loaded Electrospun PCL/PVA/CS Fiber Mats. Figure 4 shows the cumulative release of 5% owf EUG loaded into electrospun PCL/PVA/CS fiber mats produced from W/O and O/W emulsions. The release profiles revealed a burst effect of 65.05 ± 3.58% and 54.61 ± 3.19% during the initial 8 hours, followed by a continuous slow and sustained release over the next days. The observed initial burst could be due to the EUG adsorbed on or near the surface of the electrospun nanofibers, while the sustained release might be due to the diffusion of EUG from electrospun nanofibers. During the period of incubation, 80.37 ± 2.19% and 70.15 ± 1.63% of total EUG were released from W/O and O/W emulsions, respectively. This result can be explained by the higher affinity of EUG for PCL phase, which results in a faster EUG release from W/O emulsions. In addition, the EUG loaded into electrospun PCL/PVA/CS fiber mats prepared from O/W emulsion need to pass through the shell PVA/CS barrier before being released. In turn, the PVA/CS blend exhibits better wettability than the PCL and, consequently, the PVA/CS matrix is easily penetrated by the release medium, releasing the EUG quickly. Therefore, the initial EUG burst release observed is a predictable result, due to the chosen polymer blend to produce the electrospun fiber mats and selected method. The burst release can improve the therapeutic effect and accelerate the healing process, once EUG is suitable to reach some relief at the beginning of wound treatment and to stimulate an adequate initial inflammatory response, essential to proper tissue repair.

These results are in agreement with Motealleh et al. [37] in that electrospun PS fibers exhibited a lower chamomile release than electrospun PCL fibers. In this study, PCL revealed greater compatibility with the chamomile extract and its flavonoid apigenin. A similar trend was displayed by EUG loaded into W/O emulsion blend.

Controlling the rapid initial release of the biologically active compounds can be needed to treat specific types of wounds at different stages of healing. A variety of approaches have been employed to reduce and avoid the occurrence of an early burst release. Among them, the capacity of diffusion of a bioactive agent from electrospun nanofibers and the wetting properties of the electrospun nanofibers have been explored to achieve a desirable release profile. In addition, environmental factors,

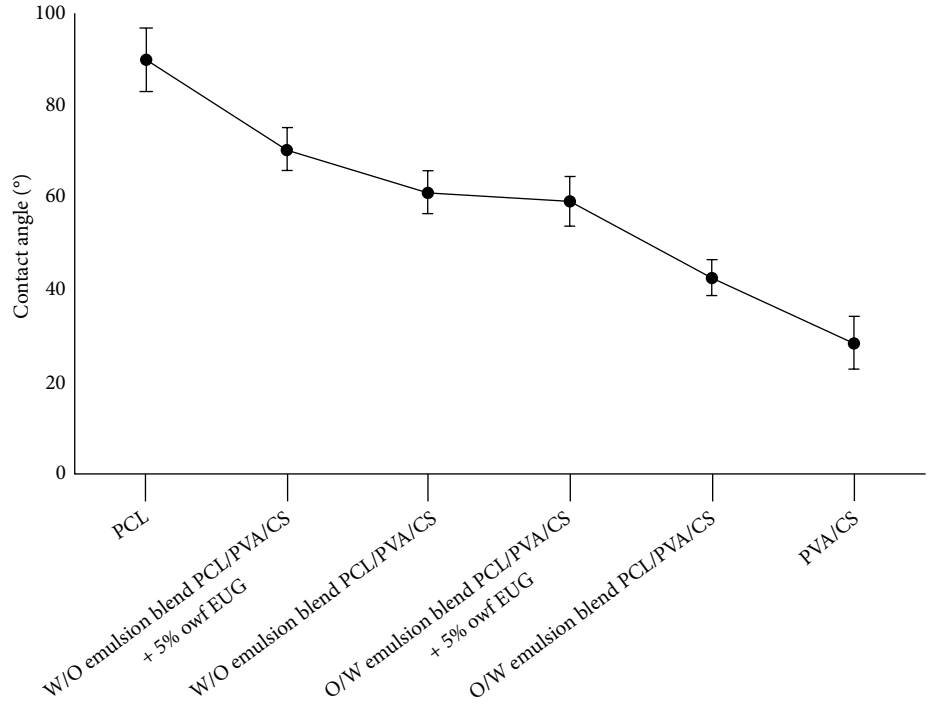

Figure 3: Variation of contact angle on pure PCL, PVA/CS and electrospun PCL/PVA/CS fiber mats prepared from W/O and O/W emulsions, with and without EUG.

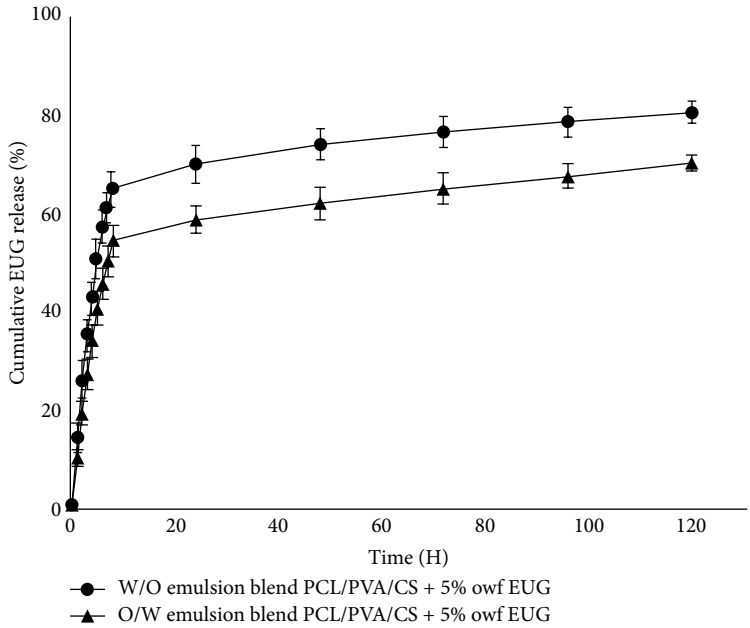

Time (h)	W/O emulsion	O/W emulsion
0	0.68 ± 0.02	0.60 ± 0.03
1	14.44 ± 3.02	10.38 ± 1.59
2	26.05 ± 4.20	19.47 ± 2.50
3	35.29 ± 3.29	27.34 ± 3.08
4	42.84 ± 3.40	34.18 ± 3.32
5	50.73 ± 4.07	40.63 ± 3.20
6	57.37 ± 3.51	45.56 ± 3.16
7	61.31 ± 3.16	50.43 ± 3.09
8	65.05 ± 3.58	54.61 ± 3.19
24	69.84 ± 3.69	58.63 ± 2.79
48	73.85 ± 3.10	61.92 ± 3.28
72	76.42 ± 3.03	64.84 ± 3.16
96	78.47 ± 2.96	67.51 ± 2.56
120	80.37 ± 2.19	70.15 ± 1.63

Figure 4: *In vitro* release study of EUG loaded into electrospun PCL/PVA/CS fiber mats at a physiological pH of 7.4 in a PBS buffer solution for 120 hours.

such as temperature, pH, or light response, have been considered as a stimulus for bioactive agent release.

3.4. Estimation of Antibacterial Activity of EUG-Loaded Electrospun PCL/PVA/CS Fiber Mats. The antibacterial efficiency of EUG loaded into electrospun PCL/PVA/CS fiber mats was quantitatively expressed as a percentage of bacterial reduction (%R) and evaluated after 24 hours against *S. aureus* and *P. aeruginosa*, two bacteria commonly present in wound infections [26].

Table 2: Antibacterial efficiency of EUG loaded into electrospun PCL/PVA/CS fiber mats against *S. aureus* and *P. aeruginosa*, expressed in percentage of bacterial reduction (%R).

Samples	*S. aureus*			*P. aeruginosa*		
		CFU/mL	Growth reduction (%)		CFU/mL	Growth reduction (%)
W/O emulsion blend PCL/PVA/CS	0 h	8.86*E*+04	—	0 h	1.77*E*+06	—
	24 h	3.04*E*+06	—	24 h	6.02*E*+07	—
W/O emulsion blend PCL/PVA/CS + 5% owf EUG		2.30*E*+05	92.43%		3.20*E*+06	94.68%
O/W emulsion blend PCL/PVA/CS	0 h	9.78*E*+04	—	0 h	2.21*E*+06	—
	24 h	2.51*E*+06	—	24 h	1.90*E*+08	—
O/W emulsion blend PCL/PVA/CS + 5% owf EUG		4.25*E*+05	83.08%		2.31*E*+07	87.85%

Table 3: Antibacterial activity values (bacteriostatic and bactericidal activity values).

Samples	*S. aureus*		*P. aeruginosa*	
	$M_B - M_C$	$M_A - M_C$	$M_B - M_C$	$M_B - M_C$
W/O emulsion blend PCL/PVA/CS + 5% owf EUG	1.12	−0.23	1.27	−0.26
O/W emulsion blend PCL/PVA/CS + 5% owf EUG	0.77	−0.64	0.92	−1.02

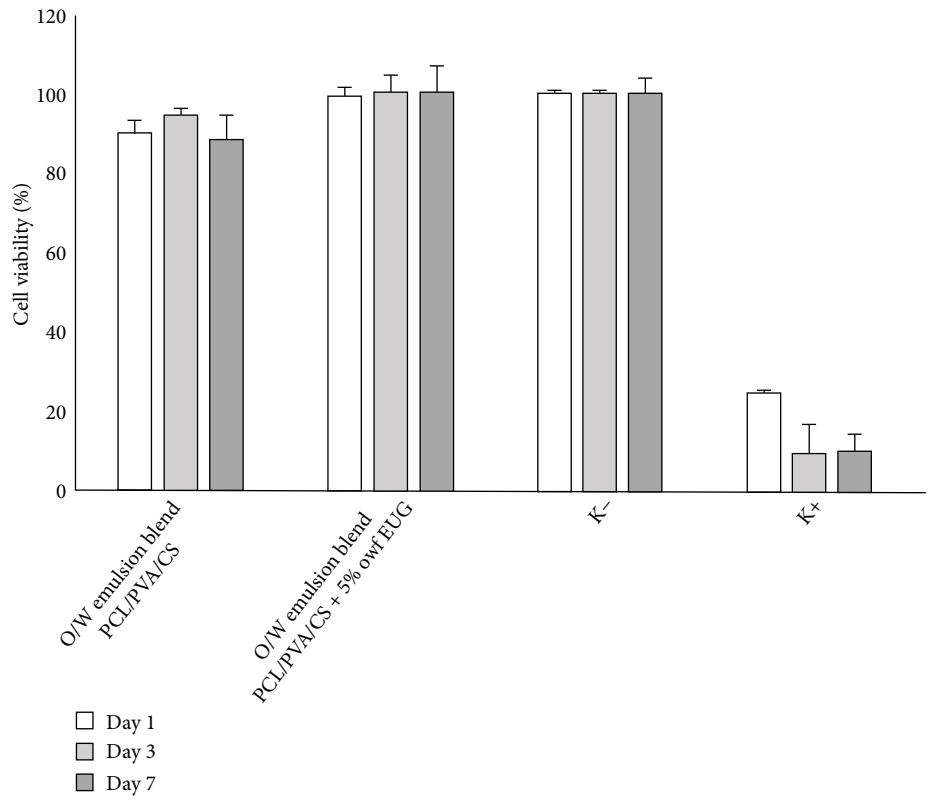

Figure 5: NHDF cell viability percentage after 1, 3, and 7 days in direct contact with the electrospun PCL/PVA/CS fiber mats prepared from O/W emulsion, with and without loaded EUG.

The results showed an inhibitory effect against selected bacteria (Table 2). Interestingly, electrospun PCL/PVA/CS fiber mats obtained from W/O emulsion revealed a higher bacterial reduction against *S. aureus* (92.43%), comparatively to O/W emulsion (83.08%). The same pattern was observed for *P. aeruginosa*. The W/O emulsion showed an increased inhibitory effect in bacterial growth (94.68%) when compared to O/W emulsion (87.85%).

These results can be explained by the difference in EUG's affinity for the polymeric blend. Such values are in agreement

with those obtained for EUG release at 24 hours (58.63 ± 2.79% from O/W emulsion and 69.84 ± 3.69% from W/O emulsion (Figure 4)), where a higher EUG release from W/O resulted in a stronger inhibition of bacterial growth.

Moreover, the electrospun PCL/PVA/CS fiber mats loaded with 5% owf EUG proved to have a bacteriostatic effect (Table 3). The bacteriostatic activity values were 1.12 and 0.77 for *S. aureus*, while for *P. aeruginosa* were 1.27 and 0.92 to W/O and O/W emulsions, respectively.

Therefore, the antibacterial efficiency of the electrospun PCL/PVA/CS fiber mats, conferred by natural properties of CS, can be strengthened with the use of EUG, as a natural antibacterial agent.

The hydrophobic nature of EUG was responsible by its mechanism of action against common pathogens present in wounds. Thus, when the EUG is partitioned into the lipid bilayer of the bacterial membrane, it changes its permeability and, consequently, rupture and release of cellular contents occur [5].

Bai et al. [38] reported the production of PCL/Chitosan nanofibers that were incorporated with tea tree oil (TTO) to improve their antibacterial ability.

3.5. Characterization of the Cytotoxicity Profile of the EUG-Loaded Electrospun PCL/PVA/CS Fiber Mats. The cytotoxic profile of the electrospun PCL/PVA/CS fiber mats with and without loaded EUG was evaluated from O/W emulsions, once these samples displayed a better capability to be applied as wound dressing materials. The results showed that the produced fiber mats did not induce any cytotoxic effect on the NHDF cells for at least 7 days, as shown in Figure 5. Moreover, the incorporation of 5% owf EUG into the emulsion blend did not compromise the cell viability. Therefore, these data reinforce the suitability of the EUG-loaded electrospun PCL/PVA/CS fiber mats for wound healing applications.

4. Conclusion

In this study, EUG, an essential oil extracted from cloves, was successfully loaded into electrospun PCL/PVA/CS fiber mats in an amount of 5% (w/w), based on the weight of PCL powder, via electrospinning from either W/O or O/W emulsion.

The results attained showed that the produced electrospun PCL/PVA/CS fiber mats with and without loaded EUG presented a high porous structure similar to the fibrous structure of native ECM. Moreover, these electrospun nanofibers exhibited surfaces with moderate wettability, which are able to provide suitable moisture at the wound site and better fibroblast attachment and proliferation. In addition, the antibacterial ability of EUG loaded into electrospun PCL/PVA/CS fiber mats was examined against *S. aureus* and *P. aeruginosa* and displayed the potential to inhibit bacterial growth.

The *in vitro* EUG release study showed a burst release of EUG in the first 8 hours, followed by a continuous slow and sustained release over the next days. The O/W emulsion revealed a better release behaviour compared to W/O emulsion, once the cumulative EUG release from W/O emulsion resulted in a faster release rate.

Therefore, the incorporation of plant essential oils, such as EUG, which exhibit unique therapeutic properties, into electrospun fiber mats from O/W emulsion revealed better results and proved to be a noncytotoxic and highly promising approach for improving the wound healing process.

Data Availability

The data used to support the findings of this study are included in the article.

Conflicts of Interest

The authors declare that they have no conflicts of interest.

Acknowledgments

The authors acknowledge the Portuguese Foundation for Science and Technology (FCT) for funding the PhD grant PD/BD/113550/2015. The manuscript was presented as a poster in the AMiCI WG2 workshop "Antimicrobial Coatings Applied in Healthcare Settings–Efficacy Testing", Berlin, Germany.

References

[1] Y. Qin, *Medical Textile Materials*, vol. 174 of *Woodhead Publishing Series in Textiles*, Woodhead Publishing, An Imprint of Elsevier, Sawston, Cambridge, UK, Waltham, MA, USA, 2016.

[2] I. Liakos, L. Rizzello, H. Hajiali et al., "Fibrous wound dressings encapsulating essential oils as natural antimicrobial agents," *Journal of Materials Chemistry B*, vol. 3, no. 8, pp. 1583–1589, 2015.

[3] R. Augustine, N. Kalarikkal, and S. Thomas, "Electrospun PCL membranes incorporated with biosynthesized silver nanoparticles as antibacterial wound dressings," *Applied Nanoscience*, vol. 6, no. 3, pp. 337–344, 2016.

[4] J. Panichpakdee, P. Pavasant, and P. Supahol, "Electrospun cellulose acetate fiber mats containing emodin with potential for use as wound dressing," *Chiang Mai Journal of Science*, vol. 43, no. 1, pp. 195–205, 2016.

[5] W. Zhang, S. Ronca, and E. Mele, "Electrospun nanofibres containing antimicrobial plant extracts," *Nanomaterials*, vol. 7, no. 2, Article ID 42, 2017.

[6] Y. Pilehvar-Soltanahmadi, M. Dadashpour, A. Mohajeri, A. Fattahi, R. Sheervalilou, and N. Zarghami, "An overview on application of natural substances incorporated with electrospun nanofibrous scaffolds to development of innovative wound dressings," *Mini-Reviews in Medicinal Chemistry*, vol. 18, no. 5, pp. 414–427, 2018.

[7] X. Hu, S. Liu, G. Zhou, Y. Huang, Z. Xie, and X. Jig, "Electrospinning of polymeric nanofibers for drug delivery applications," *Journal of Controlled Release*, vol. 185, pp. 12–21, 2014.

[8] M. R. C. Raja, V. Srinivasan, S. Selvaraj, and S. K. Mahapatra, "Versatile and synergistic potential of eugenol: a review," *Pharmaceutica Analytica Acta*, vol. 6, no. 5, pp. 367–372, 2015.

[9] X. Kong, X. Liu, J. Li, and Y. Yang, "Advances in pharmacological research of eugenol," *Current Opinion Complementary and Alternative Medicine*, vol. 1, pp. 8–11, 2014.

[10] I. B. Gomes, J. Malheiro, F. Mergulhão, J.-Y. Maillard, and M. Simões, "Comparison of the efficacy of natural-based and synthetic biocides to disinfect silicone and stainless steel surfaces", *Pathogens and Disease*, vol. 74, no. 4, Article ID ftw014, 2016.

[11] A. Moure, J. M. Cruz, D. Franco et al., "Natural antioxidants from residual sources," *Food Chemistry*, vol. 72, no. 2, pp. 145–171, 2001.

[12] K. Semnani, M. Shams-Ghahfarokhi, M. Afrashi, A. Fakhrali, and D. Semnani, "Antifungal activity of eugenol loaded electrospun PAN nanofiber mats against *Candida albicans*," *Current Drug Delivery*, vol. 15, no. 6, pp. 860–866, 2018.

[13] X. Wang, Y. Yuan, X. Huang, and T. Yue, "Controlled release of protein from core–shell nanofibers prepared by emulsion electrospinning based on green chemical," *Journal of Applied Polymer Science*, vol. 132, no. 16, Article ID 41811, 2015.

[14] S. Yan, L. Xiaoqiang, L. Shuiping, M. Xiumei, and S. Ramakrishna, "Controlled release of dual drugs from emulsion electrospun nanofibrous mats," *Colloids and Surfaces B: Biointerface*, vol. 73, no. 2, pp. 376–381, 2009.

[15] H. Qi, P. Hu, J. Xu, and A. Wang, "Encapsulation of drug reservoirs in fibers by emulsion electrospinning: morphology characterization and preliminary release assessment," *Biomacromolecules*, vol. 7, no. 8, pp. 2327–2330, 2006.

[16] M. H. El-Newehy, S. S. Al-Deyab, E.-R. Kenawy, and A. Abdel-Megeed, "Fabrication of electrospun antimicrobial nanofibers containing metronidazole using nanospider technology," *Fibers and Polymers*, vol. 13, no. 6, pp. 709–717, 2012.

[17] E. Adomaviciute, R. Milasius, and R. Levinskas, "The influence of main technological parameters on the diameter of poly(vinyl alcohol) (PVA) nanofibre and morphology of manufactured mat," *Materials Science*, vol. 13, no. 2, pp. 152–155, 2007.

[18] N. Liao, A. R. Unnithan, M. K. Joshi et al., "Electrospun bioactive poly(ε-caprolactone)-cellulose acetate-dextran antibacterial composite mats for wound dressing applications," *Colloids and Surfaces A: Physicochemical and Engineering Aspects*, vol. 469, pp. 194–201, 2015.

[19] A. Zarghami, M. Irani, A. Mostafazadeh, M. Golpour, A. Heidarinasab, and I. Haririan, "Fabrication of PEO/chitosan/PCL/olive oil nanofibrous scaffolds for wound dressing applications," *Fibers and Polymers*, vol. 16, no. 6, pp. 1201–1212, 2015.

[20] F. Ajalloueian, H. Tavanai, J. Hilborn et al., "Emulsion electrospinning as an approach to fabricate PLGA/chitosan," *BioMed Research International*, vol. 2014, Article ID 475280, 13 pages, 2014.

[21] J.-P. Chen, G.-Y. Chang, and J.-K. Chen, "Electrospun collagen/chitosan nanofibrous membrane as wound dressing," *Colloids and Surfaces A: Physicochemical and Engineering Aspects*, vol. 313, pp. 183–188, 2008.

[22] Y. Zhou, H. Yang, J. Mao, S. Gu, W. Xu, and X. Liu, "Electrospinning of carboxyethyl chitosan/poly(vinyl alcohol)/silk fibroin nanoparticles for wound dressings," *International Journal of Biological Macromolecules*, vol. 53, pp. 88–92, 2013.

[23] R. Zhang, W. Xu, and F. Jiang, "Fabrication and characterization of dense chitosan/polyvinyl-alcohol/ poly-lactic-acid blend membranes," *Fibers and Polymers*, vol. 13, no. 5, pp. 571–575, 2012.

[24] D. Liang, Z. Lu, H. Yang, J. Gao, and R. Chen, "Novel asymmetric wettable AgNPs/chitosan wound dressing. In vitro and in vivo evaluation," *ACS Applied Materials & Interfaces*, vol. 8, no. 6, pp. 3958–3968, 2016.

[25] S. Chitrattha and T. Phaechamud, "Porous poly(DL-lactic acid) matrix film with antimicrobial activities for wound dressing application," *Materials Science and Engineering C*, vol. 58, pp. 1122–1130, 2016.

[26] L. J. Bessa, P. Fazii, M. Di Giulio, and L. Cellini, "Bacterial isolates from infected wounds and their antibiotic susceptibility pattern: some remarks about wound infection," *International Wound Journal*, vol. 12, pp. 47–52, 2015.

[27] B. Tang, J. Wang, S. Xu et al., "Application of anisotropic silver nanoparticles: multifunctionalization of wool fabric," *Journal of Colloid and Interface Science*, vol. 356, pp. 513–518, 2011.

[28] N. Sanla-Ead, A. Jangchud, V. Chonhenchob, and P. Suppakul, "Antimicrobial activity of cinnamaldehyde and eugenol and their activity after incorporation into cellulose-based packaging films," *Packaging Technology and Science*, vol. 25, pp. 7–17, 2012.

[29] S. A. Mary and V. R. Giri Dev, "Electrospun herbal nanofibrous wound dressings for skin tissue engineering," *The Journal of the Textile Institute*, vol. 106, no. 8, pp. 886–895, 2015.

[30] J. Hu, M. P. Prabhakaran, X. Ding, and S. Ramakrishn, "Emulsion electrospinning of polycaprolactone: influence of surfactant type towards the scaffold properties," *Journal of Biomaterials Science, Polymer Edition*, vol. 26, no. 1, pp. 57–75, 2015.

[31] T. Briggs and T. L. Arinzeh, "Examining the formulation of emulsion electrospinning for improving the release of bioactive proteins from electrospun fibers," *Journal of Biomedical Materials Research Part A*, vol. 102, no. 3, pp. 674–684, 2014.

[32] H. Hajiali, M. Summa, D. Russo et al., "Alginate–lavender nanofibers with antibacterial and anti-inflammatory activity to effectively promote burn healing," *Journal of Materials Chemistry B*, vol. 4, no. 9, pp. 1686–1695, 2016.

[33] A. Gholipour-Kanani, S. H. Bahrami, and S. Rabbani, "Effect of novel blend nanofibrous scaffolds on diabetic wounds healing," *IET Nanobiotechnology*, vol. 10, pp. 1–7, 2016.

[34] M. M. Lim, T. Sun, and N. Sultana, "In vitro biological evaluation of electrospun polycaprolactone/gelatine nanofibrous scaffold for tissue engineering," *Journal of Nanomaterials*, vol. 2015, Article ID 303426, 10 pages, 2015.

[35] J. Cui, L. Qiu, Y. Qiu, Q. Wang, and Q. Wei, "Co-electrospun nanofibers of PVA-SbQ and zein for wound healing," *Journal of Applied Polymer Science*, vol. 132, no. 39, Article ID 42565, 2015.

[36] S. Maretschek, A. Greiner, and T. Kissel, "Electrospun biodegradable nanofiber nonwovens for controlled release of proteins," *Journal of Controlled Release*, vol. 127, no. 2, pp. 180–187, 2008.

[37] B. Motealleh, P. Zahedi, I. Rezaeian, M. Moghimi, A. H. Abdolghaffari, and M. A. Zarandi, "Morphology, drug release, antibacterial, cell proliferation, and histology studies of chamomile-loaded wound dressing mats based on electrospun nanofibrous poly(E-caprolactone)/polystyrene blends," *Journal of Biomedical Materials Research Part B*, vol. 102, no. 5, pp. 977–987, 2014.

[38] M.-Y. Bai, T.-C. Chou, J.-C. Tsai, and W.-C. Yu, "The effect of active ingredient-containing chitosan/polycaprolactone nonwoven mat on wound healing: *In vitro* and *in vivo* studies," *Journal of Biomedical Materials Research Part A*, vol. 102, no. 7, pp. 2324–2333, 2014.

Hindawi
Advances in Polymer Technology
Volume 2019, Article ID 5727536, 10 pages
https://doi.org/10.1155/2019/5727536

Research Article

Estimation of Volatile Organic Compounds (VOCs) and Human Health Risk Assessment of Simulated Indoor Environment Consisting of Upholstered Furniture Made of Commercially Available Foams

Alena Capíková,[1] Daniela Tesařová,[2] Josef Hlavaty,[2] Adam Ekielski,[3] and Pawan Kumar Mishra [4]

[1]*Textile Testing Institute, Brno, Czech Republic*
[2]*Department of Furniture, Design, and Habitat, Mendel University in Brno, Zemědělská 1665/1, 613 00 Brno-sever-Černá Pole, Brno, Czech Republic*
[3]*Department of Production Management and Engineering, Warsaw University of Life Sciences, Warsaw, Poland*
[4]*Department of Wood Processing Technology, Mendel University in Brno, Zemědělská 1665/1, 613 00 Brno-sever-Černá Pole, Brno, Czech Republic*

Correspondence should be addressed to Pawan Kumar Mishra; xmishra@mendelu.cz

Received 25 April 2019; Accepted 31 July 2019; Published 9 October 2019

Guest Editor: Bin Xu

This study was conducted for the qualitative and quantitative determination of volatile organic compounds (VOCs) and total volatile organic compounds (TVOC) from polymeric foam materials used in upholstered furniture. Six different types of foams viz. Highly elastic foam K5040, standard PU foam N5063, bonded polyurethane foam R100, viscoelastic foam V5020, self-extinguishing foam KF5560, and foam rubber were used. Short-term and long-term (24, 48, 72, 672 hours (28 day)) measurements were done to differentiate the role of primary emissions (present in new products) and secondary emissions (due to chemical reactions in material or slowly released due to the porous structure of material). The samples were collected using a small-space sampling chamber at a temperature of 23°C and a humidity of 50% depending on the aspect of time. The concentrations of VOC and TVOC were identified and quantified using a Gas chromatography–Mass spectroscopy (GC-MS) based method. Based on the VOC measurements, the standard room concentrations were simulated to estimate the human health risk assessment for all six types of foams. The results of simulations suggest no possibility of human health risk for the very long period (28 days), as the estimated values were found to be much below the prescribed limits.

1. Introduction

Today's society spends the majority of their time in confined spaces, mostly in their homes, up to 95% and about 6% of their time in vehicles [1]. The indoor environment is, therefore, an important aspect of human life, and it is essential that its quality—health safety—is at the highest level. Air quality can be measured and analyzed by taking an air sample, which is evaluated by the appropriate method for the amount of volatile organic substances (VOC) and total volatile organic compounds (TVOC) ranging from hexane to hexadecane (C6–C16) which is an indicator of ambient air cleanliness. The primary sources of emissions in the interior are furniture materials like the wood used in furniture [2, 3], foams, and human activities. The most widespread compounds are formaldehyde and acetaldehyde. The reason for their wide occurrence is their volatile character and the fact that they are widely used in the production of a large number of household products such as paints, lacquers, waxes, solvents, and detergents. They have also been shown to be emitted during the use of electronic devices such as printers, copiers, and others [4]. Concerns about consumer safety are a reason to control airborne pollutants like VOCs, and these undesirable substances are released from the materials used in indoor products manufacturing [5]. Several technologies have been developed to address this issue [6]. There are several other polymers like lignin and cellulose (in wood), and their

Table 1: Parameters of various samples used in the study.

Material	Density ($kg\,m^{-3}$)	Cell diameter	Manufacturer and supplier
Highly elastic foam K5040	46.5–51.5	3 mm	Eurofoam GmbH (Austria) and BPP spol s.r.o, Czech Republic
Standard PU foam N5063	46.5–51.5	0.8–1.5 mm	Eurofoam GmbH (Austria) and BPP spol s.r.o., Czech Republic
Bonded polyurethane foam R 100	90–120	—	Eurofoam GmbH (Austria) and BPP spol s.r.o, Czech Republic
Viscoelastic foam V5020	45–55	—	Eurofoam GmbH (Austria) and BPP spol s.r.o, Czech Republic
Self-extinguishing foam KF5560	51.5–59.5	—	Eurofoam GmbH (Austria) and BPP spol s.r.o, Czech Republic
Foam rubber	—	—	Eurofoam GmbH (Austria) and BPP spol s.r.o., Czech Republic

derivatives present in different indoor product formulations that can adsorb and retain the VOCs, but this study is more focused on upholstered furniture [7–10].

On average, one-third life of a person is spent by sleeping [11]. This is the time spent not only in bed but also on resting furniture such as upholstered sofas, where the lying area (seating area) is composed of foamed materials (called as polyurethane foams (PU) or foam rubber (LATEX name). These polymer-based materials have a cellular structure and are therefore porous and hence, to a certain extent, breathable. It performs the softening function of the touch surfaces with the body of the user, and at the same time, it can behave as a carrier of VOCs. Generally, VOCs can be controlled at source (during the manufacturing of the indoor product), ventilation, and air-cleaning [12]. The reported methods for air-cleaning include botanical purification, Catalytic combustion, Membrane Separation, Zeolite based adsorption, Bio-filtration, Absorption, and activated carbon-based adsorption [13–15]. Every method has its advantages and disadvantages, and the best suitable method can vary from site to site. In the context of upholstered furniture, properties of foam can be modified by additives, novel blowing agents and new biobased polymers or at least minimised within prescribed limits [16, 17].

In a previous study, the potential risks of VOCs released from five types of polyurethane foams by simulating the scenario of a man lying on a soft foam mattress for 8 h/day were estimated [18], in which, the measurements for very long-term intervals were missing that limited the data availability about passive emissions. In this study, six commonly used foams in upholstered furniture (commercially available) were characterized for their permeability and emitted VOCs. Measurements were done at the interval of 24, 48, 72, and 672 h (28 days) intervals. Long-term measurements (28 days) were done to differentiate the primary emissions (physically released compounds present in new products) and secondary emissions (compounds produced by a chemical reaction in a product or in the microstructure and are released gradually). This study aims to provide the missing data about secondary emissions that take relatively long time to be emitted. Based on VOC values from our experiment, the concentration of VOCs in a standard room was modeled to assess Human health risk for all six types of materials.

2. Materials

The internal used standards were from ethylacetate, toluene, hexanal, *n*-butyl acetate, ethylbenzene, *m*,*p*-xylene, styrene, *o*-xylene, *α*-pinene, 3-ethyltoluene, *D*-10-*o*-xylene, 1,2,4-trimethylbenzene (Supelco, Sigma Aldrich), 3-*δ*-carene and butoxyethanol (Fluka). The parameters of samples tested for VOC content can be found in Table 1. The size of the measured sample was $0.65\,m \times 0.65\,m \times 0.05\,m$, $S = 0.98 m^3$.

3. Methodology

3.1. Sampling of Released VOCs. Prior to VOC measurement, each sample was air-conditioned for 72 h by placing it in a small-space emission chamber. The concentration of VOCs released was assessed at different intervals of time using ISO 16000-9, (2006) standards [19]. Foam samples were placed in a hermetically sealed space of defined temperature 23°C, relative atmospheric humidity of 50%, and air velocity of 0.1 to $0.3\,ms^{-1}$. Sampling for analysis was collected using a small volume space chamber VOC TEST 1000 with a volume of $1\,m^3$. The sampling was carried out via a splitter by pumping air through two pumps with an airflow of $12\,l.h^{-1}$ through two sorption tubes with Tenax TA sorbent, where the organic components were adsorbed on the sorbent. The time of one sampling was 180 min. Measurement of the individual polymeric foam materials loaded with emissions for the analysis of TVOC and VOC was performed by a 24 h, 48 h, 72 h, and 672 h (28 days) intervals.

3.2. GC-MS System and Analysis of Samples. The samples collected in Tenax Tube were subjected to thermal desorption system, from where they were injected into Gas Chromatography with a mass spectrometry system equipped with the ChemStation program. The content of the sorption sampling tube is desorbed using thermal desorption from the tube into a column of capillary column gas-chromatograph and a mass-spectrometer detector (Figure 1). Subsequently, qualitative and quantitative data are evaluated using ChemStation software. The internal standard D10-*o*-xylene method is used for evaluation according to ISO 16000-6, (2011) [20]. The MS-SPL–BOTH method (MS-mass spectrometry, SPL-Splitless Injection Method; BOTH-collection of all ions SCAN (scanning all ions within a given weight range) and selected ions SIM (single for selected ion monitoring) in the spectrum), which works in two modes simultaneously SCAN and SIM, was used to analyze samples of air samples of tested materials (Table 2). The RT retention time, target ion Tg and control ions Q1, Q2, and Q3 in SIM mode are used to identify individual VOCs. The target ion peak areas (Tg) are designed to evaluate the concentration of individual VOCs. The peak

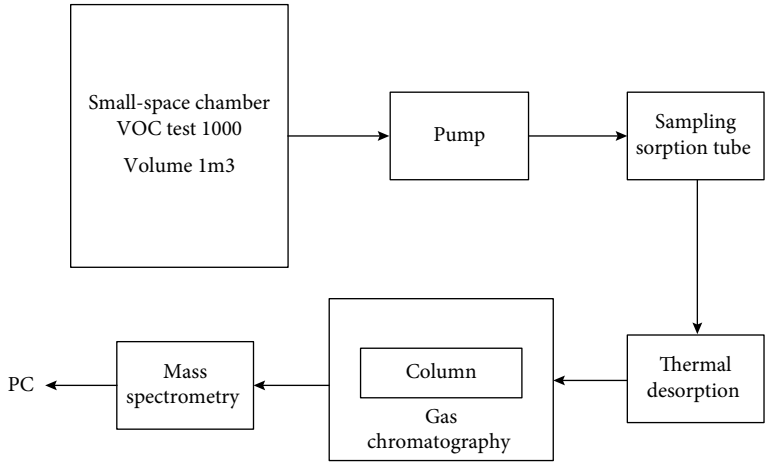

Figure 1: Flow chart of the various steps in VOC measurements.

areas in the total ionic ion chromatogram (TIC) are used to evaluate the TVOC. Calculate the content of VOCs and TVOC first by using ChemStation software, where we obtain the amount of analyte in ng per tube. Conversion to weight concentration is performed in Excel. The SCAN mode serves to evaluate the TVOC parameter. TVOC is the sum of all VOC compounds that are eluted from the chromatographic column between *n*-hexane and *n*-hexadecane including these.

3.3. Estimations of Human Health Risk. To assess human health risk, the worst scenario was modeled using the measured values of VOCs. The worst scenario was based on the maximum measured concentration of the compound irrespective of the time. Previously reported equations and methodology were used to assess the health risk in s standard room. These estimated values were then compared with the value of the NOAEL and PEL (if available). This gave an idea of health risk possibilities in a standard room. Upholstered furniture (modular sofa) with total surface area 12.81 m^2 was assumed to be placed in a standard room of volume 30 m^3. All surfaces were assumed to be emitting the VOCs to model the worst scenario. Following equations were used for modeling purpose as reported by Hillier et al. [18].

$(A_s : A_k)$: area of sample in standard room and chamber, 12.81 m^2–0.98 m^2

$(V_s : V_k)$: volume of standard room and chamber, 30 m^3–1 m^3

$(n_s : n_k)$: air change in standard room and chamber, 0.5 h^{-1}–1 h^{-1}

$(L_s : L_k)$: area specific volume flow in a standard room and chamber, $L = A/V$

C_s calculated the concentration of the volatile chemical in a standard room

C_k measured the concentration of a volatile chemical in the test chamber

$$C_s = C_k \times (n_k/n_s) \times (A_s/A_k) \times (V_k/V_s), \quad (1)$$

$$C_s = C_k \times (1/0.5) \times (12.81/0.98) \times (1/30), \quad (2)$$

$$C_s = C_k \times (2) \times (13.07) \times (0.0333), \quad (3)$$

$$C_s = C_k \times 0.87. \quad (4)$$

Thus, the concentration of volatile chemical in a standard room is the product of concentration of volatile chemical in the test chamber multiplied by 0.87.

4. Results and Discussions

The sources of VOCs in the indoor environment can be paints, furniture, appliances and decorative item. There are three levels of this problem handling source, ventilation, and air cleaning. Several methods have been reported to control VOCs in the indoor environment such as toluene adsorption using activated carbon [15, 23], catalytic or UV methods [22], an additive in foam formulation [17], thermal oxidation, and bio-treatment [13, 14] methods. Every method comes with its advantages and limitations that should be considered based on individual indoor conditions. However, this manuscript is focused on polymeric foams and health risk assessment in indoor condition by their emitted VOCs. The measured TVOC values for individual materials are presented in Figure 2. It can be seen in Figure 2 that the TVOC values were observed to be relatively high for K5040, V5020, and foam rubber materials as compared to the others. However, a time-dependent decrease in TVOC content was not observed in all materials. It also suggests the role of secondary emission and its variation based on the material properties (porosity and permeability). Additionally, the presented results indicate that the values of TVOC for K5040, N5063, and foam rubber decreased over time. While, KF 5560, R100, and V5020 behaved differently over time and did not confirm a decrease in TVOC over time. In KF5560, we can see a gradual small increase in TVOC over time, up to 72 h (241 $\mu g\,m^{-3}$), which after 672 h dropped sharply to 109 $\mu g\,m^{-3}$. Similarly, the TVOC values for V5020 gradually increased to the 326 $\mu g\,m^{-3}$ in 48 h, followed by a negligible decrease to 323 $\mu g\,m^{-3}$ in 72 and ultimately decreasing to 138 $\mu g\,m^{-3}$ in 672 h. The R100 material showed a decrease in TVOC values upto 102 $\mu g\,m^{-3}$ in 72 h. However, post 672 h, the value is increased to 148 $\mu g\,m^{-3}$. It is where the role of

Table 2: Thermal desorption and GC-MS parameters used in the study.

Thermal desorption	Short Path Thermal Desorption Controller model TD–4, Serial J210		
	Temperature and time conditions of thermal desorption		
Operation	Time (s)	Temperature (°C)	
Gas purge time	300	–	
Injection time	30	–	
Desorption time	180	200 (initial)–250 (final)	
GC start delay	30		
Gas chromatograph	Agilent Technologies GC 6890 Network GC System		
Mass spectrometry	Agilent Technologies GC 6890 Network GC System		
	Thermostat		
Initial temp (°C)	40		
Initial time (min)	2		
	Temperature rise rate (°C.min^{-1})	Final temp (°C)	Final time (min)
Ramp	8	240	20
Run time (min)	47	47	47
	Front Inlet		
Mode	Split		
Temp ($^{\circ}$C)	250		
Pressure (kPa)	62,9		
Split ratio	40:1		
Split flow (mL.min^{-1})	47,9		
Total flow (mL.min^{-1})	52,6		
Gas type	Helium		
	Column		
Capillary column type:	AGILENT HP–5MS (5% Phenyl methyl siloxane)		
Max. temperature (°C)	325		
Nominal length (m)	30		
Nominal diameter (μm)	250		
Nominal film thickness (μm)	1		
Initial flow (mL.min^{-1})	1,2		
Average velocity (cm.sec^{-1})	40		
Nominal init pressure (kPa)	63		
Outlet	MSD		
Outlet pressure	vacuum		
	Zone MS		
MS Quad–temp (°C)	150 (max 200)		
MS Source–temp (°C)	230 (max 250)		
Acquisition Mode	SCAN/SIM		
Low mass	25		
High mass	500		
Threshold	50		

secondary emissions can be assumed to cause anomalous behaviour.

In post-24-hour measurements, all materials showed TVOC above 300 μg m^{-3}, except for KF5560 at 180 μg m^{-3}. The highest concentrations were measured after 24 h for K5040, N5063, foam rubber and R100 foamed polyurethane foams. The viscoelastic foam V5020 reached the highest concentration of 323 µg m^{-3} and the polyurethane foam with flame-retardants KF5560 reached the highest concentration of 216 µg m^{-3} for 48 h measurements. The highest concentration after 72 h was observed for viscoelastic foam V5020 (323 μg m^{-3}). For K5040, KF5560, foam rubber, the concentration for 72 h ranged from 211 to 256 μg m^{-3}. The lowest concentration values after 72 h were measured in the bound polyurethane foam R100 102 μg m^{-3} and polyurethane foam N5063 124 μg m^{-3}. The lowest concentration of 97 μg m^{-3} after 672 h was found in N5063. The highest concentration of 229 μg m^{-3} after 672 h was detected in K5040. In the case of the arithmetic mean of the TVOCs found over a total period of measurement time for the materials, we can divide these materials into three groups according to the average result value. The first group is materials that released over time over

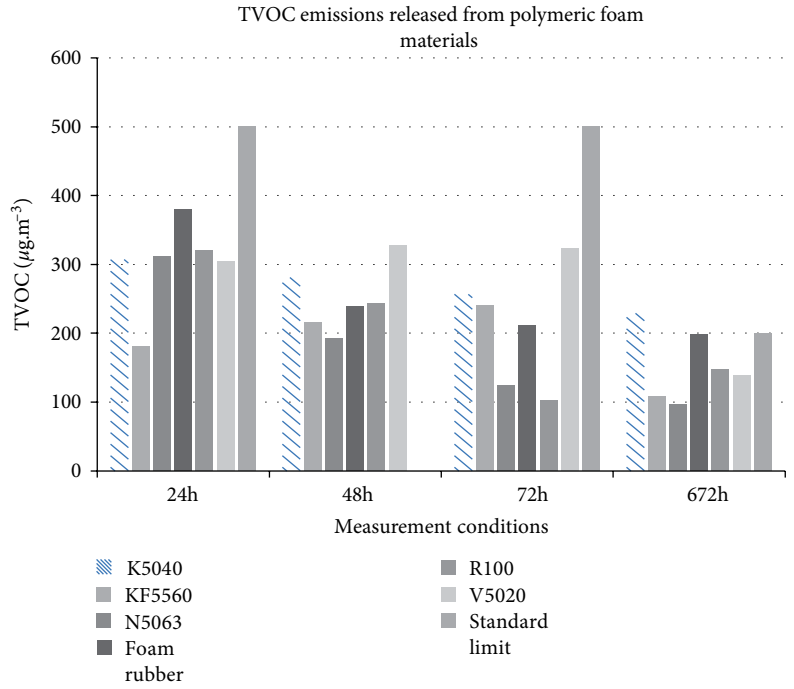

Figure 2: Measured TVOC concentrations for different foams with respect to time. (standard limits as per [21, 22], limits for 48 h not available)

100 μg m^{-3} TVOC is K5040 and R100. The second group is materials that have released TVOC over 90 μg m^{-3}, is foam rubber, N5063 and V5020 over time. Moreover, the third group is materials that released TVOC below 90 μg m^{-3} is KF5560 over time.

In the analysis of the identified VOCs, 13 significant substances were measured as presented in Figure 3. The highest concentration of the monitored determinant was observed for toluene (26.6 μg m^{-3}) in the bound polyurethane foam R100 for 24 h measurements. Significant concentrations of 18 μg m^{-3} were also measured with foam rubber for 24 h. The toluene was found to be in a higher concentration for all materials as compared to other substances. The lowest concentration of 3 μg m^{-3} after 24 h was detected in the viscoelastic foam V5020. The least loaded material with toluene is the viscoelastic foam V5020. The most burdened material with toluene is the bonded polyurethane foam R100. Individual concentrations of toluene gradually decrease concerning time for all measured materials.

Another compound that showed a high concentration of 19.3 μg m^{-3} in foam rubber and 17.8 μg m^{-3} in the bound polyurethane foam R100 after 24 h was *m*,*p*-xylene. The lowest concentration of 8.9 μg m^{-3} over 24 h was detected in the viscoelastic foam V5020. Although *m*,*p*-xylene has not reached as high concentrations as toluene in the individual foam analysis, it has, compared to other high concentrations over time, individual materials over time. The *m*-*p*-xylene was released in minimum quantity by the V5020 viscoelastic foam. The most releasing material for *p*-xylene was a bonded polyurethane foam R100. Concentrations of *m*,*p*-xylene gradually decrease over time in all measured materials. The substance ethyl acetate was detected in a higher concentration above 1 μg m^{-3} only in the bound R100 foam polyurethane foam. Hexanal was the most representative of K5040 polyurethane foam over time; the highest concentration reached 672 h. Hexanal not only reduces but also increases as observed in K5040 polyurethane foam, foam rubber, and bonded R100 polyurethane foam.

N-Butyl acetate showed the highest concentrations in foam rubber and the R100 polyurethane foam after 672 h and therefore did not decrease with time; this also can be attributed to secondary emissions. Ethylbenzene reached the highest concentration of 10.7 μg m^{-3} in the N5063 polyurethane foam after 24 h, with concentrations lower than 1 μg m^{-3} after 48 h–672 h. It was significantly accentuated with time for K5040 polyurethane foam, foam rubber and bonded R100 polyurethane foam. The concentration of styrene was observed to be decreasing with time for K5040 polyurethane foam, foam rubber, and bonded R100 polyurethane foam. *O*-xylene showed the highest concentration of 8.3 μg m^{-3} in foam rubber after 24 h. It was followed by a decrease with time. A similar trend was observed in all other samples too, except viscoelastic foam V5020. *O*-xylene concentration showed a decrease over time for all types of tested samples. For butoxyethanol, the highest concentration reached 3.6 μg m^{-3} in foam rubber for 672 h. No decrease in concentration was observed with time. 3-δ-Caren at was measured above 1 μg m^{-3} after 24 h, 48 h, 72 h, and 672 h in foam rubber only. The highest concentration was reached after 72 h.

None of the measured TVOC values of individual materials exceeded the Ecolabel and CertiPUR label requirements, where the concentration of volatile organic compounds should not exceed 500 μg m^{-3}. In the simulated health risk assessment, none of the compounds showed a value higher than prescribed

Table 3: The measured and simulated concentrations of VOCs and limits.

Volatile	Test chamber highest conc K5040	Standard room highest conc K5040	Test chamber highest conc KF5560	Standard room highest conc KF5560	Test chamber highest conc N5063	Standard room highest conc N5063	Test chamber highest conc foam rubber [$\mu g/m^3$]	Standard room highest conc foam rubber	Test chamber highest conc R100	Standard room highest conc R100	Test chamber highest conc V5020	Standard room highest conc V5020	Limit	Source of limit
Ethylacetate	0,10	0,09	0,30	0,26	0,20	0,17	0,20	0,17	2,50	2,18	0,00	0,00	70 000	PEL/10
Toluene	13,00	11,31	7,50	6,53	10,70	9,31	18,00	15,66	26,60	23,14	3,00	2,61	191	NOAEL
Hexanal	1,90	1,65	0,50	0,44	2,00	1,74	1,70	1,48	1,20	1,04	0,60	0,52	394	NOAEL
n-Butyl acetate	2,60	2,26	1,20	1,04	1,10	0,96	6,40	5,57	5,20	4,52	1,10	0,96	–	–
Ethylbenzene	3,10	2,70	3,70	3,22	10,70	9,31	4,80	4,18	5,10	4,44	2,40	2,09	20 000	PEL/10
m,*p*-Xylene	11,00	9,57	14,10	12,27	12,90	11,22	19,30	16,79	17,80	15,49	8,90	7,74	20 000 (all xylene)	PEL/10
Styrene	2,20	1,91	1,80	1,57	2,00	1,74	3,00	2,61	2,20	1,91	1,10	0,96	85 000	NOAEL
o-Xylene	4,70	4,09	6,40	5,57	5,80	5,05	8,30	7,22	7,00	6,09	4,50	3,92	20 000 (all xylene)	PEL/10
Butoxyethanol	2,30	2,00	1,60	1,39	0,40	0,35	3,60	3,13	0,80	0,70	1,50	1,31	10 000	PEL/10
α-Pinene	0,20	0,17	0,10	0,09	0,10	0,09	1,10	0,96	0,50	0,44	0,10	0,09	–	–
3-Ethyltoluene	1,10	0,96	0,70	0,61	0,40	0,35	1,10	0,96	0,20	0,17	1,10	0,96	–	–
1,2,4-Trimethylbenzene	0,50	0,44	0,50	0,44	0,70	0,61	1,00	0,87	0,30	0,26	0,40	0,35	10 000	PEL/10
3-δ-Carene	1,10	0,96	1,20	1,04	1,40	1,22	2,90	2,52	1,40	1,22	0,80	0,70	–	–

The NOAEL is defined as "no observed adverse effect level". PEL is defined as Acceptable Exposure Limits in Working Environment according to Government Decree no. 361/2007 Coll.

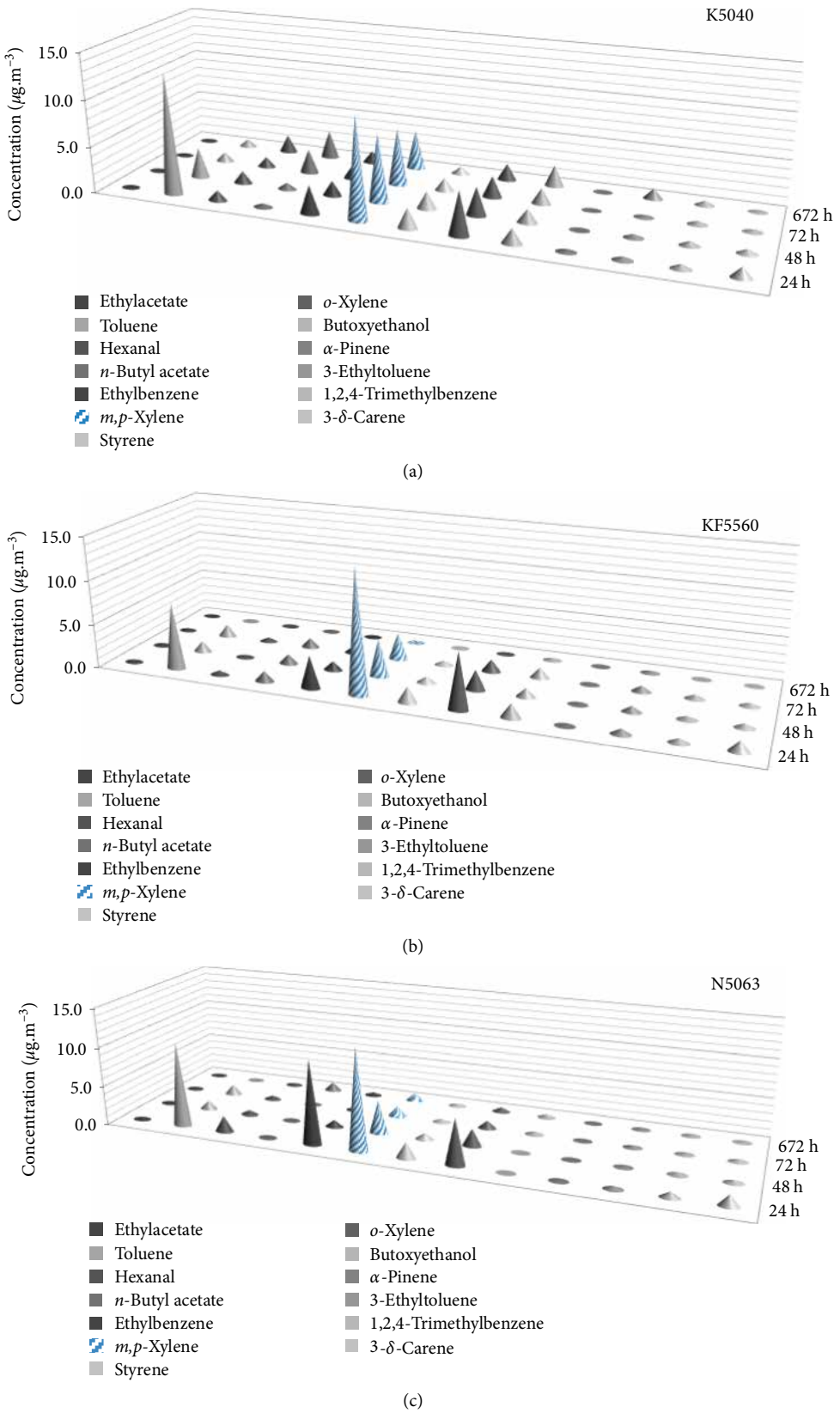

Figure 3: Continued.

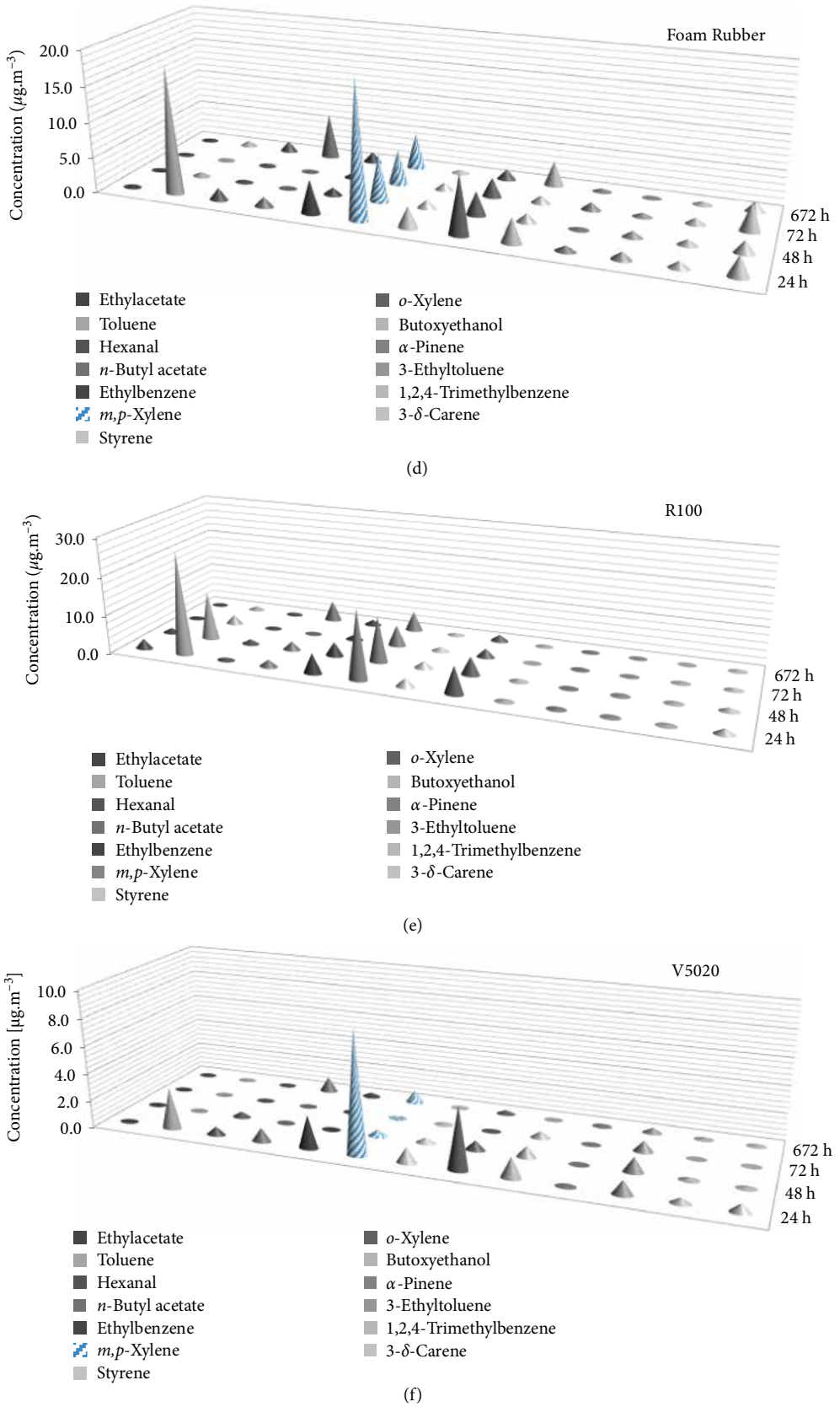

Figure 3: Concentration of Different VOCs emitted by different foams with time.

limits; thereby no health risk could be suggested (Table 3). The maximum simulated value was observed for Toluene in R100 with 23.14 $\mu g/m^3$ that too was much below the prescribed values by NOEL.

5. Conclusion

VOCs are released from materials in different ways over time. Therefore, we can not say that in time the concentration decreases if we take the order of the individual measurements after 24 h, 48 h, 72 h,and 672 h in the determined VOCs or the peak area decreases for the identified VOCs. As a result, the values after 672 h are much lower than after 24 h. However, not for all measured materials, we can see that the concentration of the VOC peak would be lower than the initial 24-hour measured concentration. Thus, over a longer period, the concentration or peak area decreases compared to the initial measurement. In the case of individual polymeric foam materials, the comparison of the concentrations in the decreasing order, ethylacetate, toluene, hexanal, *n*-butylacetate, ethylbenzene, *m*,*p*-xylene, styrene, *o*-xylene, butoxyethanol, 3-ethyltoluene, 1,2,4-trimethylbenzene, 3-δ-carene. As observed, the comparison of the peak area, the decreasing order follows as, 1,4-dimethylpiperazine, 4-ethylmorpholine, triethylenediamine, *N*,*N*-dimethylbenzene-methanamine, undecane, 2-ethylhexanoic acid, decamethylcyclo-pentasiloxane, dodecane, tridecane, and dodecamethylcyclohexasiloxane.

It can be concluded that it is difficult to generalize the time-dependent decrease in VOC release with time for all kind of polymers as these values vary on time, material, and individual VOC basis. However, in simulated values, it can be seen that none of the studied VOCs was observed to be even near the prescribed limit. Hence zero health risk can be suggested. Considering the variation in source dependent nature and quantity of TVOC cocktail and in toxicity level of individual compound, it is suggested to minimise their content at different possible levels. Various formulation strategies for foams with functional additives in addition to the modified fabrics should be utilised to minimise VOC emissions.

Data Availability

The datasets generated during and/or analyzed during the current study are available from the corresponding author on reasonable request.

Conflicts of Interest

The authors declare that they have no conflicts of interest.

Acknowledgments

The authors are grateful for the support of the Technology Agency of Czech Republic; grant number TH03030416 through the project "Progresivní konstrukce a řízení sušáren pro těžko sušitelné dřeviny včetně exotických" for the financial support.

References

[1] P. Pluschke and H. Schleibinger, *Indoor Air Pollution - Part F*, Springer, Spain, 2018, https://www.springer.com/gb/book/9783662560631.

[2] D. Tesarova, P. Cech, E. Jeřábková et al., "Effect of ethylene oxide sterilization and accelerated ageing on the physical and mechanical properties of beech, oak, and elm wood: part 2," *BioResources*, vol. 13, no. 4, 2018.

[3] D. Tesařová, A. Capíková, E. Jeřábková, P. Čech, A. Ekielski, and P. K. Mishra, "Effect of ethylene oxide sterilization and accelerated ageing on the physical and mechanical properties of beech, oak, and elm wood: part 1," *BioResources*, vol. 13, no. 4, 2018.

[4] D. A. Sarigiannis, S. P. Karakitsios, A. Gotti, I. L. Liakos, and A. Katsoyiannis, "Exposure to major volatile organic compounds and carbonyls in European indoor environments and associated health risk," *Environmental International*, vol. 37, no. 4, pp. 743–765, 2011.

[5] H. Mishra, P. K. Mishra, A. Ekielski, M. Jaggi, Z. Iqbal, and S. Talegaonkar, "Melanoma treatment: from conventional to nanotechnology," *Journal of Cancer Research and Clinical Oncology*, vol. 144, no. 12, pp. 2283–2302, 2018.

[6] P. K. Mishra, K. Giagli, D. Tsalagkas et al., "Changing face of wood science in modern era: contribution of nanotechnology," *Recent Patents Nanotechnology*, vol. 12, no. 1, pp. 13–21, 2018.

[7] P. K. Mishra and A. Ekielski, "The self-assembly of lignin and its application in nanoparticle synthesis: a short review," *Nanomaterials*, vol. 9, no. 2, p. 243, 2019.

[8] P. K. Mishra and R. Wimmer, "Aerosol assisted self-assembly as a route to synthesize solid and hollow spherical lignin colloids and its utilization in layer by layer deposition," *Ultrasonics Sonochemistry*, vol. 35, pp. 45–50, 2017.

[9] J. Bhandari, H. Mishra, P. K. Mishra, R. W. Wimmer, F. J. Ahmad, and S. Talegaonkar, "Cellulose nanofiber aerogel as a promising biomaterial for customized oral drug delivery," *International Journal of Nanomedicine*, vol. 12, pp. 2021–2031, 2017.

[10] P. K. Mishra and A. Ekielski, "A simple method to synthesize lignin nanoparticles," *Colloids and Interfaces*, vol. 3, no. 2, p. 52, 2019.

[11] J. Laverge, A. Novoselac, R. Corsi, and A. Janssens, "Experimental assessment of exposure to gaseous pollutants from mattresses and pillows while asleep," *Building and Environment*, vol. 59, pp. 203–210, 2013.

[12] Y. Huang, S. S. H. Ho, Y. Lu et al., "Removal of indoor volatile organic compounds via photocatalytic oxidation: a short review and prospect," *Molecules*, vol. 21, no. 1, p. 56, 2016.

[13] S. Lau, K. Groody, A. Chan, and G. Ragib, "Control of reduced sulphur and VOC emissions via biofiltration," *Pulp and Paper Research journal*, vol. 107, pp. 57–63, 2006.

[14] T. P. Kumar, M. Rahul, and B. Chandrajit, "Biofiltration of volatile organic compounds (VOCs): an overview," *Research Journal of Chemical Science*, vol. 2231, p. 606X, 2011.

[15] A. Mofidi, H. Asilian, and A. J. Jafari, "Adsorption of volatile organic compounds on fluidized activated carbon bed," *Health Scope*, vol. 2, pp. 84–89, 2013.

[16] N. Adam, G. Avar, H. Blankenheim et al., "Polyurethane," *Ullmann's Encyclopedia of Industrial Chemistry*, 2005.

[17] J. J. Burdeniuc, J. D. Tobias, and R. J. Keller, "Process for producing flexible polyurethane foam using natural oil polyols," 2012, Patent EP12735726.7A.

[18] K. Hillier, T. Schupp, and I. Carney, "An investigation into VOC emissions from polyurethane flexible foam mattresses," *Cellular Polymers*, vol. 22, no. 4, pp. 237–259, 2003.

[19] ISO 16000-9, *Indoor Air-Part 9: Determination of the Emission of Volatile Organic Compounds from Building Products and Furnishing-Emission Test Chamber Method*, International Organization for Standardization, 2006.

[20] ISO 16000-6, *Indoor Air–Part 6: Determination of Volatile Organic Compounds in Indoor and Test Chamber Air by Active Sampling on Tenax TA Sorbent, Thermal Desorption and Gas Chromatography Using MS/FID*, International Organization for Standardization, 2011.

[21] B. Guieysse, C. Hort, V. Platel, R. Munoz, M. Ondarts, and S. Revah, "Biological treatment of indoor air for VOC removal: potential and challenges," *Biotechnology Advances*, vol. 26, no. 5, pp. 398–410, 2008.

[22] S. Wang, H. M. Ang, and M. O. Tade, "Volatile organic compounds in indoor environment and photocatalytic oxidation: state of the art," *Environment International*, vol. 33, no. 5, pp. 694–705, 2007.

[23] M. P. Cal, M. J. Rood, and S. M. Larson, "Removal of VOCs from humidified gas streams using activated carbon cloth," *Gas Separation & Purification*, vol. 10, no. 2, pp. 117–121, 1996.